IOWA STATE UNIVERSITY
Digital Repository

Retrospective Theses and Dissertations

Iowa State University Capstones, Theses and Dissertations

1969

The response of a coupled core reactor to a localized oscillation of the absorption cross section

Walter Charles Nodean
Iowa State University

Follow this and additional works at: https://lib.dr.iastate.edu/rtd

 Part of the Nuclear Engineering Commons, and the Oil, Gas, and Energy Commons

Recommended Citation
Nodean, Walter Charles, "The response of a coupled core reactor to a localized oscillation of the absorption cross section " (1969). *Retrospective Theses and Dissertations*. 4136.
https://lib.dr.iastate.edu/rtd/4136

This Dissertation is brought to you for free and open access by the Iowa State University Capstones, Theses and Dissertations at Iowa State University Digital Repository. It has been accepted for inclusion in Retrospective Theses and Dissertations by an authorized administrator of Iowa State University Digital Repository. For more information, please contact digirep@iastate.edu.

www.manaraa.com

70-13,616

NODEAN, Walter Charles, 1940-
THE RESPONSE OF A COUPLED CORE REACTOR TO A LOCALIZED OSCILLATION OF THE ABSORPTION CROSS SECTION.

Iowa State University, Ph.D., 1969
Engineering, nuclear

University Microfilms, Inc., Ann Arbor, Michigan

THIS DISSERTATION HAS BEEN MICROFILMED EXACTLY AS RECEIVED

THE RESPONSE OF A COUPLED CORE REACTOR TO A LOCALIZED OSCILLATION OF THE ABSORPTION CROSS SECTION

by

Walter Charles Nodean

A Dissertation Submitted to the
Graduate Faculty in Partial Fulfillment of
The Requirements for the Degree of
DOCTOR OF PHILOSOPHY

Major Subject: Nuclear Engineering

Approved:

Signature was redacted for privacy.

In Charge of Major Work

Signature was redacted for privacy.

Head of Major Department

Signature was redacted for privacy.

Dean of Graduate College

Iowa State University
Ames, Iowa
1969

TABLE OF CONTENTS

I. INTRODUCTION

In order to control a nuclear reactor properly, it is necessary to know the response of the reactor to reactivity perturbations. Because of this, the study of reactor response has been an integral part of the developing reactor technology, and it is the topic of this thesis.

The response of a reactor is usually given in terms of the reactor transfer function (30, 38). The transfer function of any system is defined as the Laplace transform of the output divided by the Laplace transform of the input. For a reactor, the input is a reactivity perturbation and the output is usually taken to be the change in the neutron flux. Because it lends itself well to both analytical and experimental treatment, one of the most common methods of determining the transfer function of a reactor is to introduce into the reactor, while it is in a steady-state condition, a sinusoidally varying reactivity perturbation, usually as a variation in the absorption cross section, and then to determine the resultant flux change. When this is done, it is found (38) that the flux also varies sinusoidally with the same frequency as the input, but with a different amplitude and phase. This frequency response is the magnitude and phase angle of the reactor transfer function.

A reactor concept which is becoming increasingly important in the light of recent developments, such as the

consideration being given to the idea of clustered nuclear rocket engines, is the coupled-core nuclear system. A coupled-core reactor has two or more distinct fuel regions or cores, and they are coupled in the sense that some of the neutrons produced in one core will diffuse to another core and cause fissions there and vice versa. As Avery (3) has pointed out, this concept could be applied to the separate fuel elements in any reactor, but it is usually advantageous to do so only when each core itself has an appreciable multiplication factor and is physically separated from the other cores by a non-multiplying medium. Intuitively, it can be seen that the frequency response of a coupled-core reactor might be different from that of a single-core reactor, and it is the purpose of this thesis to propose a method for determining that response.

In order to determine the frequency response of a reactor analytically it is necessary to develop a reasonably accurate model of the reactor. For many reactors, the spatially independent or point-kinetics equations (30) give an adequate representation of the flux, and when the first transfer function measurements were made in 1952 by Harrer et al. (21) on the CP-2, good agreement was obtained with their point kinetics model at the low frequencies ($\leq$ 20 rad/sec) they investigated. However, as reactors have become larger and more complex, it has been necessary to

include spatial effects when developing a reactor model. Some of the early work done in this area was that of Henry and Curlee (22) who proposed, in 1958, to handle spatial effects by approximating neutron shape functions with a series of time-independent calculations (a forerunner of the time-synthesis technique). Since then, several different techniques have been proposed to approximate the spatially-dependent flux, examples of which are given by Kaplan (26), Kaplan et al. (28), and Lewins (33).

By far the most popular method of approximating the spatially-dependent flux has been the modal analysis approach. In this method, it is assumed that the flux can be approximated by the sum of a series of products of space-dependent expansion modes and time-dependent coefficients. The problem is then to select appropriate space modes and solve for the time coefficients. Many different space modes have been proposed, but they can all be divided into two basic types: the orthogonal modes, which are eigenfunctions of the steady-state problem, and the non-orthogonal modes. The orthogonal modes include the Helmholtz modes (16, 17), the lambda and omega modes (28), and the natural modes (25). The non-orthogonal modes include the Green's function modes (15) and the time-synthesis modes (27, 29). In general, it is arbitrary which type of space mode is used, but one type of space mode may be better suited for a particular problem

than another type; that is, the series of one type may converge faster than that of another type.

As the different reactor models have been developed, they have been used to determine the spatially-dependent frequency response. The first attempt to determine this response was made in 1948 by Weinberg and Schweinler (39) who investigated only very low frequencies. Since that time, in most of the analytic work done in this area, the diffusion equations have been used as the model (32, 34), with approximate solutions to them being obtained. Cohn et al. (12) have proposed a complex formulation and have used it with a time-synthesis approach; Hoshino et al. (24) have formulated a method based on the modal expansion technique; and Foulke and Gyftopoulos (18) have used the natural mode approximation to find the response of a model of the heavy-water NORA reactor. The only published experimental results of frequency response measurements are those of Hansson and Foulke (20) who also investigated the NORA reactor.

The first model for a coupled-core reactor was proposed by Avery (3) in 1958. He wrote a point-kinetics equation for each core which included coupling terms to account for the diffusion of neutrons from core to core. A somewhat similar technique was proposed by Baldwin (4) who wrote a one-group diffusion equation, including coupling terms, for

each core. Much of the work done on coupled-core reactors (6, 36) has utilized the idea of treating each core as a point, but recently, Yasinsky (42) has proposed a method for finding spatial effects by utilizing a time-synthesis approach.

Little work has been published on the frequency response of coupled-core reactors. Pluta (36), utilizing Avery's method (3), investigated the response at low frequencies ($\leq$ 10 rad/sec); Seale (37), using Baldwin's method (4), investigated a three-core system for frequencies up to 10^4 rad/sec; and Carter and Danofsky (9) made the first study of the spatially-dependent frequency response by approximating the flux with Green's function modes.

The purpose of this thesis is to present a method for determining the spatially dependent frequency response of a coupled-core reactor. The particular reactor chosen for study is the Iowa State University UTR-10 (1), a description of which is given in Appendix A. Frequency response work which has been done for the UTR-10 includes that of Danofsky and Uhrig (14), Betancourt (7), and Merrit (35). To find the spatially-dependent frequency response, Betancourt used the natural mode approximation and Merrit used the Green's function mode approximation developed by Carter (8). The results obtained by Betancourt and Merritt will be compared to the results obtained here.

The method presented here consists of casting the two group diffusion equations into the form of linear differential equations which can be solved exactly by the use of the Green's function technique (13, 23). In order to do this, it is assumed that the reactor power is low enough so that no feedback (temperature, etc.) occurs. This method is similar to that used by Banks and Blackshaw (5) and Kobayashi and Nishihara (31) to obtain steady-state flux distributions.

This method is considered to be an improvement over the modal analysis techniques since it does give an essentially exact solution to the diffusion equations.

II. THEORY OF THE GREEN'S FUNCTION SOLUTION TO A DIFFERENTIAL EQUATION

This section presents a review of the theory of the Green's function solution to a differential equation which is used in the following sections to solve the diffusion equations. This review is based on material in Courant and Hilbert (13) and Hildebrand (23).

The problem to be considered is solving the differential equation

$$Ly(x) + \Phi(x) = 0 \quad , \tag{1}$$

where L is the linear, self-adjoint, differential operator

$$L = \frac{d}{dx}(p\frac{d}{dx}) + q = p\frac{d^2}{dx^2} + \frac{dp}{dx}\frac{d}{dx} + q \quad , \tag{2}$$

together with homogeneous boundary conditions over the region of interest--that is, in the region $a \leq x \leq b$, $y(a) = y(b) = 0$. The assumptions are made that in this region p, $\frac{dp}{dx}$, and q are continuous functions of x and that p is not zero.

If a unit perturbation is introduced at some point ε, where $a < \varepsilon < b$, the effect of that perturbation at some other point x can be denoted as $G(x,\varepsilon)$. Thus, the effect at x of the continuously distributed perturbation Φ can be considered to be the superposition of the effects of an infinite number of point perturbations, and the desired

solution will have the form

$$y(x) = \int_a^b G(x,\varepsilon)\Phi(\varepsilon)d\varepsilon \quad . \tag{3}$$

The function $G(x,\varepsilon)$ is called the Green's function, and for a given number ε, is given by $G_1(x)$ for $x < \varepsilon$ and by $G_2(x)$ for $x > \varepsilon$. The Green's function satisfies the following conditions:

1. $G(x,\varepsilon)$ satisfies the equation $LG = 0$; that is, $LG_1 = 0$ when $x < \varepsilon$ and $LG_2 = 0$ when $x > \varepsilon$.
2. $G(x,\varepsilon)$ satisfies the prescribed homogeneous boundary conditions; that is, $G_1(a) = 0$ and $G_2(b) = 0$.
3. $G(x,\varepsilon)$ is continuous at $x = \varepsilon$; that is, $G_1(\varepsilon) = G_2(\varepsilon)$.
4. The first derivative of $G(x,\varepsilon)$ has a discontinuity of magnitude $-1/p(\varepsilon)$ at $x = \varepsilon$; that is,

$$\frac{dG_2(\varepsilon)}{dx} - \frac{dG_1(\varepsilon)}{dx} = -1/p(\varepsilon).$$

The four conditions listed are used to determine G. Let $c_1u(x)$ be a nontrivial solution to $LG = 0$ which satisfies the boundary condition at $x = a$; that is, $u(a) = 0$. Also, let $c_2v(x)$ be a nontrivial solution to $LG = 0$ which satisfies the boundary condition at $x = b$; that is, $v(b) = 0$. c_1 and c_2 are constants. The first two conditions are then satisfied if $G_1 = c_1u(x)$ and $G_2 = c_2v(x)$, so that

$$G = \begin{cases} c_1 u(x) , & x < \varepsilon \\ c_2 v(x) , & x > \varepsilon \end{cases} \quad . \tag{4}$$

c_1 and c_2 are determined by using the last two conditions. By Condition 3

$$c_1 u(\varepsilon) = c_2 v(\varepsilon) \quad \text{or} \quad c_2 v(\varepsilon) - c_1 u(\varepsilon) = 0 \quad . \tag{5}$$

By Condition 4

$$c_2 \frac{dv(\varepsilon)}{dx} - c_1 \frac{du(\varepsilon)}{dx} = -1/p(\varepsilon) \quad . \tag{6}$$

Equations 5 and 6 possess a unique solution if

$$\begin{vmatrix} u(\varepsilon) & v(\varepsilon) \\ \frac{du(\varepsilon)}{dx} & \frac{dv(\varepsilon)}{dx} \end{vmatrix} = u(\varepsilon)\frac{dv(\varepsilon)}{dx} - v(\varepsilon)\frac{du(\varepsilon)}{dx} \neq 0 \quad .$$

This determinant, called the Wronskian, will not be zero unless u(x) and v(x) are linearly dependent. If that is the case, a Green's function in the normal sense will not exist. For this exceptional case a generalized Green's function can be defined, but since it is not relevant to the development here, it will not be discussed further. The value of the Wronskian for the normal case in which u(x) and v(x) are linearly independent can be found by noting that both u(x) and v(x) satisfy Ly = 0. Therefore,

$$\frac{d}{dx}\left(p\frac{du}{dx}\right) + qu = 0$$

and

$$\frac{d}{dx}(p\frac{dv}{dx}) + qv = 0 .$$

Multiplying the second equation by u and the first equation by v and subtracting the results yields

$$u\frac{d}{dx}(p\frac{dv}{dx}) - v\frac{d}{dx}(p\frac{du}{dx}) = \frac{d}{dx}[p(u\frac{dv}{dx} - v\frac{du}{dx})] = 0 .$$

Thus,

$$p(u\frac{dv}{dx} - v\frac{du}{dx}) = A ,$$

where A is a constant. Thus, the value of the Wronskian is

$$u(\varepsilon)\frac{dv(\varepsilon)}{dx} - v(\varepsilon)\frac{du(\varepsilon)}{dx} = \frac{A}{p(\varepsilon)} . \qquad (7)$$

With this relationship, the solutions of Equations 5 and 6 become

$$c_1 = -\frac{v(\varepsilon)}{A} , \qquad c_2 = -\frac{u(\varepsilon)}{A} .$$

Thus, Equation 4 becomes

$$G(x,\varepsilon) = \begin{cases} -\dfrac{u(x)v(\varepsilon)}{A} , & x < \varepsilon \\ -\dfrac{u(\varepsilon)v(x)}{A} , & x > \varepsilon \end{cases} .$$

[In an actual problem for the solution of a Green's function, u(x), v(x), and p(x) will be known; so that A can be evaluated from Equation 7.]

Using the definition of the Green's function as given

above, it can be shown, using only the elementary rules for the differentiation of an integral with respect to a parameter, that Equation 3 is completely equivalent to Equation 1. Thus, Equation 3 is the solution of Equation 1 and satisfies the boundary conditions.

This method of solving a differential equation by using the Green's function is not limited to second order equations. An analogous procedure can be used in solving a boundary-value problem consisting of a differential equation of order n and relevant homogeneous boundary conditions. Considering the equation

$$Ly(x) + \Phi(x) = 0 \quad , \tag{8}$$

where now L is an n^{th} order differential operator, the corresponding Green's function,

$$G(x,\varepsilon) = \begin{cases} G_1(x) & , \quad x < \varepsilon \\ G_2(x) & , \quad x > \varepsilon \end{cases} ,$$

satisfies the following conditions:

1. For $x < \varepsilon$, G_1 satisfies the equation $LG_1 = 0$. For $x > \varepsilon$, G_2 satisfies the equation $LG_2 = 0$.
2. Over the interval (a,b), G_1 satisfies the prescribed homogeneous boundary condition at a, and G_2 satisfies the corresponding condition at b.

3. $G(x,\varepsilon)$ and its first n-2 x-derivatives are continuous at $x = \varepsilon$.
4. The $(n-1)^{th}$ x-derivative of $G(x,\varepsilon)$ has a discontinuity of magnitude $-1/s(x)$ at $x = \varepsilon$, where $s(x)$ is the coefficient of d^n/dx^n in L.

These are the generalized conditions for a Green's function, and it is readily seen that those conditions given previously are merely the application of these to a second-order equation. Under these conditions the solution to Equation 8 can again be written as

$$y(x) = \int_a^b G(x,\varepsilon)\Phi(\varepsilon)d\varepsilon \quad .$$

A special case of particular interest is when the driving function $\Phi(x)$ is a delta function; that is,

$$\Phi(x) = \delta(x-x') \quad , \quad a < x' < b \quad .$$

In this case the solution, Equation 3, becomes

$$y(x) = \int_a^b G(x,\varepsilon)\delta(\varepsilon-x')d\varepsilon = G(x,x') \qquad (9)$$

since

$$\delta(x-x') = \begin{cases} \infty \ , & x = x' \\ 0 \ , & x \neq x' \end{cases} \quad \text{and} \quad \int_a^b \delta(x-x')dx = 1 \quad .$$

Thus, if $\mathfrak{P}(x)$ is a delta function, the desired solution is identical with the Green's function, and the integration step is bypassed completely.

III. APPLICATION OF THE GREEN'S FUNCTION THEORY TO A SLAB REACTOR

In utilizing the theory of the Green's function to determine the spatially dependent frequency response of a reactor, a bare, homogeneous, semi-infinite, slab reactor was investigated first. One-group theory, with one group of delayed neutrons, was used to keep the model simple. Table 1 (2) contains the critical nuclear parameters for this reactor.

Table 1. Slab reactor parameters

D(cm)	$\Sigma_a(cm^{-1})$	$\Sigma_f(cm^{-1})$	Neutron velocity (cm/sec)	$\tau(cm^2)$
0.2712	0.09235	0.0591	2.2×10^5	42
Thickness of slab (cm)	β	$\lambda\ (sec^{-1})$	ν	$B^2(cm^{-2})$
30	0.0064	0.08	2.5	0.010966

With these parameters the reactor is exactly critical, which is very important; because it was found that, especially at low frequencies, the frequency response of this reactor (and also the UTR-10 model) is very sensitive to criticality.

A sinusoidal variation in the absorption cross section Σ_a was assumed to occur in a plane at the exact center of the reactor. In an actual experimental set-up this could be approximated by using a small neutron-absorber oscillator.

The basic diffusion equations are

$$D\frac{d^2}{dx^2}\phi - \Sigma_a\phi + \nu\Sigma_f(1-\beta)e^{-B^2\tau}\phi + \lambda Ce^{-B^2\tau} = \frac{1}{v}\frac{\partial\phi}{\partial t} \qquad (10)$$

$$\nu\Sigma_f\beta\phi - \lambda C = \frac{\partial C}{\partial t} \quad , \qquad (11)$$

where the symbols have their usual meanings. The term $e^{-B^2\tau}$ accounts for the leakage of fast neutrons. With a small perturbation in Σ_a,

$$\Sigma_a = \Sigma_{ao} - \Delta\Sigma_a \quad , \qquad (12a)$$

then

$$\phi = \phi_o + \Delta\phi \qquad (12b)$$

and

$$C = C_o + \Delta C \quad . \qquad (12c)$$

Σ_{ao}, ϕ_o, and C_o are the steady-state values. Substituting Equations 12 into Equations 10 and 11, noting that the steady-state parts of the equations sum to zero, and assuming the product $\Delta\Sigma_a\Delta\phi$ is negligibly small, leads to the resultant equations

$$D\frac{d^2}{dx^2}\Delta\phi - \Sigma_{ao}\Delta\phi + \Delta\Sigma_a\phi_o + \nu\Sigma_f(1-\beta)e^{-B^2\tau}\Delta\phi + \lambda\Delta C = \frac{1}{v}\frac{\partial\Delta\phi}{\partial t} \tag{13}$$

$$\nu\Sigma_f\beta\Delta\phi - \lambda\Delta C = \frac{\partial\Delta C}{\partial t} \quad . \tag{14}$$

As stated, the perturbation $\Delta\Sigma_a$ was assumed to be sinusoidal and to occur in a plane. This can be expressed mathematically as

$$\Delta\Sigma_a = \lim_{\gamma\to o}\frac{1}{2\gamma}\{U_1(x-[x'-\gamma])-U_2(x-[x'+\gamma])\}|\Delta\bar{\Sigma}_a|e^{j\omega t} \quad ,$$

where U_1 and U_2 are unit step functions,

x' = location of oscillator in the reactor,

γ = small unit of length,

$|\Delta\bar{\Sigma}_a| = (2\gamma)(\Delta\Sigma_a)$ which is the total absorption probability of the oscillator (39),

ω = frequency of oscillator,

and

$j = \sqrt{-1}$.

As γ approaches zero the expression

$$\frac{1}{2\gamma}\{U_1(x-[x'-\gamma]) - U_2(x-[x'+\gamma])\}$$

becomes identical with $\delta(x-x')$(41); therefore

$$\Delta\Sigma_a = \delta(x-x')|\Delta\bar{\Sigma}_a| e^{j\omega t} . \quad (15a)$$

Thus,

$$\Delta\phi = \Delta\hat{\phi}(x,\omega)e^{j\omega t} \quad (15b)$$

and

$$\Delta C = \Delta\hat{C}(x,\omega)e^{j\omega t} , \quad (15c)$$

where $\Delta\hat{\phi}$ and $\Delta\hat{C}$ are the complex amplitudes of $\Delta\phi$ and ΔC respectively.

After substituting Equations 15 into Equations 13 and 14 and dividing out the common factor $e^{j\omega t}$, the resultant equations are

$$D\frac{d^2}{dx^2}\Delta\hat{\phi} - \Sigma_{ao}\Delta\hat{\phi} + \delta(x-x')|\Delta\bar{\Sigma}_a|\phi_o + \nu\Sigma_f(1-\beta)e^{-B^2\tau}\Delta\hat{\phi}$$

$$+ \lambda\Delta\hat{C}e^{-B^2\tau} = \frac{j\omega}{v}\Delta\hat{\phi} \quad (16)$$

$$\nu\Sigma_f\beta\hat{\Delta\phi} - \lambda\hat{\Delta C} = j\omega\hat{\Delta C} \quad . \tag{17}$$

Solving Equation 17 for $\hat{\Delta C}$ and substituting into Equation 16 yields

$$\frac{d^2}{dx^2}\hat{\Delta\phi} + B_m^2\hat{\Delta\phi} + \frac{|\bar{\Delta\Sigma}_a|\phi_o}{D}\delta(x-x') = 0 \quad , \tag{18}$$

where

$$B_m^2 = \frac{1}{D}\left[-\Sigma_{ao} + \nu\Sigma_f(1-\beta)e^{-B^2\tau} + \frac{\lambda\nu\Sigma_f\beta e^{-B^2\tau}}{\lambda + j\omega} - \frac{j\omega}{v}\right] \quad .$$

Equation 18 has the same form as Equation 1 with the driving function Φ equal to

$$\frac{|\bar{\Delta\Sigma}_a|\phi_o}{D}\delta(x-x') \quad .$$

Thus, the solution for $\hat{\Delta\phi}$ can be obtained by the Green's function method; and since Φ is a delta function, the solution is

$$\hat{\Delta\phi} = \frac{|\bar{\Delta\Sigma}_a|\phi_o}{D}G(x,x') \quad , \tag{19}$$

where G is the Green's function.

To obtain the Green's function it is necessary to apply the four conditions listed in Section II. Thus, from the first condition

$$\frac{d^2}{dx^2}G + B_m^2G = 0 \quad . \tag{20}$$

The solution to Equation 20 can be obtained by using the ordinary techniques for solving a differential equation (41). Thus,

$$G_1 = A_1 e^{jB_m x} + A_2 e^{-jB_m x} \quad , \quad x < x'$$

$$G_2 = A_3 e^{jB_m x} + A_4 e^{-jB_m x} \quad , \quad x > x' \quad .$$

The A_i are determined by applying the remaining conditions on the Green's function; that is,

$$G_1 = 0 \quad \text{at} \quad x = 0 \quad ,$$

$$G_2 = 0 \quad \text{at} \quad x = 30 \text{ cm} \quad ,$$

$$G_1 = G_2 \text{ at } x = x' = 15 \text{ cm} \quad ,$$

and

$$\frac{dG_2}{dx} - \frac{dG_1}{dx} = -1 \quad \text{at} \quad x = x'$$

since $p(x') = 1$. These conditions lead to a system of four simultaneous, algebraic equations in the A_i from which the values of the A_i can be found. Thus, the solutions for $\hat{\Delta\emptyset}$ are (from Equation 19)

$$\hat{\Delta\emptyset} = \frac{|\bar{\Delta\Sigma}_a|\emptyset_o}{D}[A_1 e^{jB_m x} + A_2 e^{-jB_m x}] \text{ for } x < x' \qquad (21a)$$

$$\hat{\Delta\emptyset} = \frac{|\bar{\Delta\Sigma}_a|\emptyset_o}{D}[A_3 e^{jB_m x} + A_4 e^{-jB_m x}] \text{ for } x > x' \quad . \qquad (21b)$$

Since the solutions for $\hat{\Delta\phi}$ (Equations 21) are continuous in x, it is possible to find the frequency response at any point in the reactor. Since $\hat{\Delta\phi}$ is complex, it can be written as $\hat{\Delta\phi} = a + jb$, where a and b are real numbers. With this definition, the magnitude or gain of the response in decibels is

$$\text{Mag.} = 20 \log_{10}\sqrt{a^2 + b^2} \quad , \tag{22a}$$

and the phase angle in degrees is

$$\text{Phase} = \frac{180}{\pi} \left(\tan^{-1} \frac{b}{a}\right) \quad . \tag{22b}$$

In solving for $\hat{\Delta\phi}$ it is necessary to obtain the square root of the complex number B_m^2, where B_m^2 can be written as $c + jd$ [c and d are real numbers]. The method used was that of Churchill (10); that is,

$$B_m = \sqrt{r}\left[\cos\frac{\theta + 2\pi k}{2} + j \sin\frac{\theta + 2\pi k}{2}\right] \quad , \quad k = 0,1,$$

where

$$r = \sqrt{c^2 + d^2} \qquad \text{and} \qquad \theta = \tan^{-1} \frac{d}{c} \quad .$$

This method was used because it is more accurate, especially at low frequencies, than the subprogram for obtaining complex square roots available from the computer.

The results obtained for the frequency response of this slab reactor are shown in Figures 1 and 2. Although some space dependence can be seen, many similarities are evident

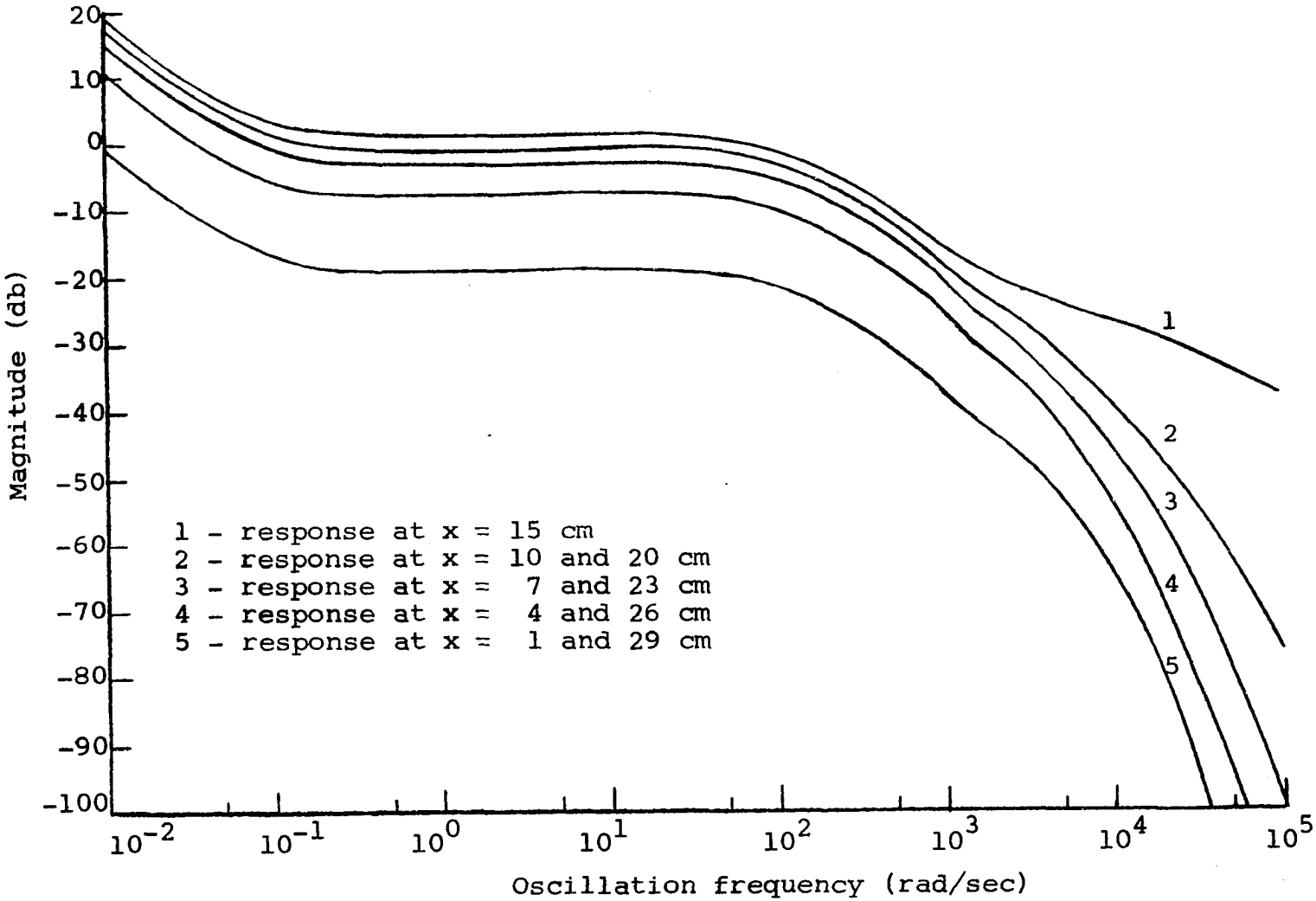

Figure 1. Magnitude of frequency response in slab reactor

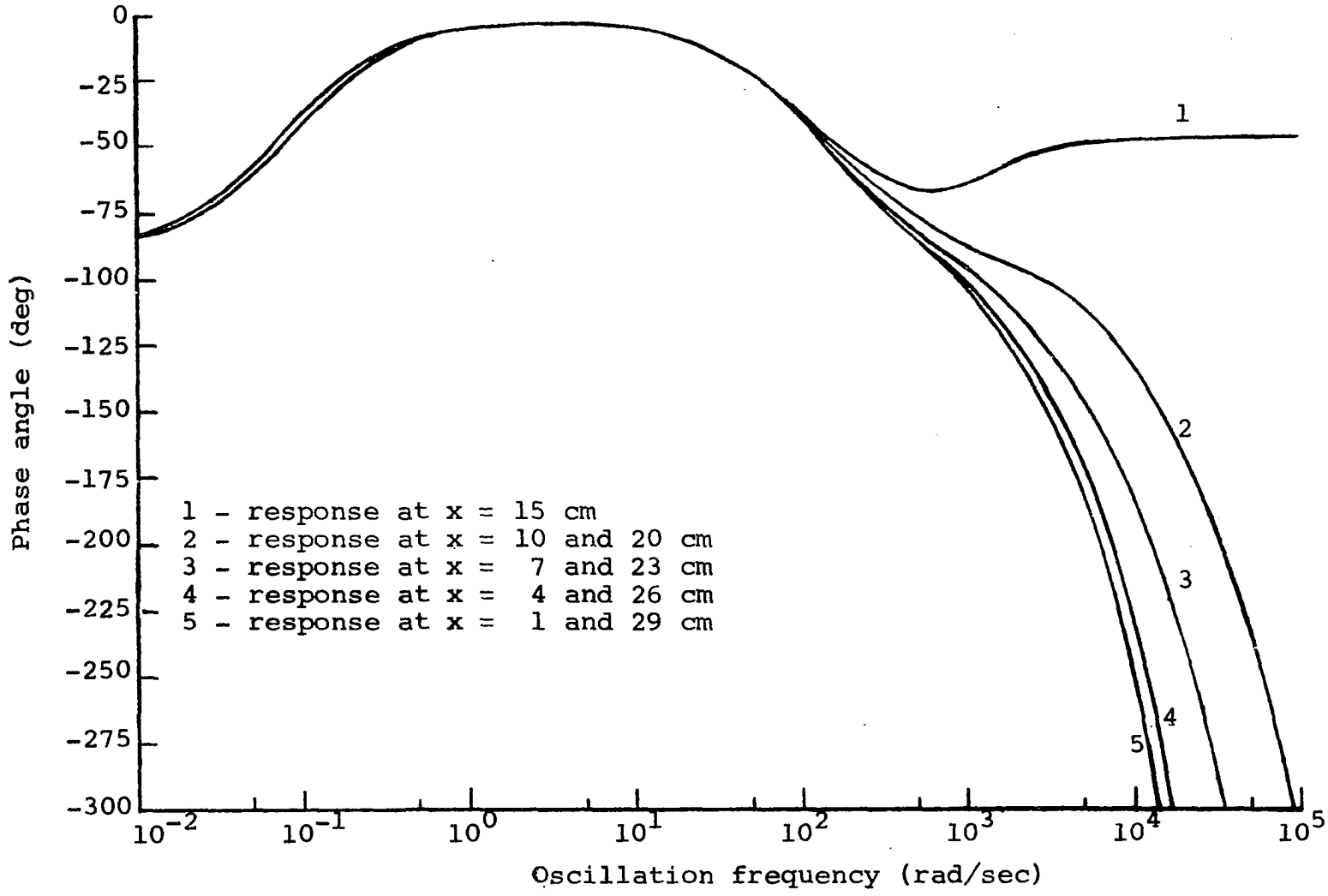

Figure 2. Phase of frequency response in slab reactor

between these results and the space independent case. The transfer function as derived from the point kinetics equations is (38)

$$\frac{n_o(j\omega + \lambda)}{j\omega\Lambda(j\omega + \beta/\Lambda)} ,$$

where Λ is the neutron lifetime. For this reactor, Λ is 4.76×10^{-5} sec (2). A magnitude plot of the space independent transfer function would indicate break frequencies at λ and β/Λ. For this reactor, $\lambda = 0.08$ and $\beta/\Lambda = 134$ which agree very closely with the break frequencies in the results shown. In fact, below a frequency of about 500 rad/sec these results are almost identical with the space independent case which is as expected. Similarly, the phase angle response is almost identical with the space independent response below 500 rad/sec. The space dependence of the results is evident mostly in the difference in the response at the position of the oscillator and at all other positions. The gain at the position of the oscillator decreases much less rapidly with increasing frequency than at the other positions, and the phase angle at the oscillator position asymptotically approaches -45° with increasing frequency whereas at the other positions the phase angle continuously decreases. This phase angle response at high frequencies for all positions is the greatest departure from the space

independent case in which the phase angle asymptotically approaches -90° at high frequencies. The difference in the response at the oscillator position is probably due to a resonance effect in which the effect of the neutron perturbation is being reflected back to the source of the perturbation. The frequency response is symmetric about the center of the reactor as expected.

IV. APPLICATION OF THE GREEN'S FUNCTION THEORY TO THE UTR-10 MODEL

A. Description of UTR-10 Model

In developing a model of the UTR-10 reactor, some simplifications were made, but it is felt that the results are still representative of the actual UTR-10. Danofsky and Uhrig (14) and Merritt (35) have shown that the flux tilt in the UTR-10 has a negligible effect on the frequency response; therefore this model was developed with no flux tilt, which greatly simplified the calculations. The two-group diffusion equations with one group of delayed neutrons, Equations B.1 - B.3 of Appendix B, were taken as the basis for this model. In using these equations, it is assumed that there is no absorption of fast neutrons and only slow neutrons cause fissions. A one-dimensional analysis was performed, but the transverse buckling was used to account for the neutron leakage through the top, bottom, and two sides of the reactor. The value of the transverse buckling has been found by Merritt (35), who made a horizontal and vertical flux map through a core tank, extrapolated the fluxes to zero, and obtained the buckling in each direction by assuming the flux obeyed equations of the form

$$\phi(y) = A_1 \sin B_y y$$

$$\phi(z) = A_2 \sin B_z z \quad .$$

The total transverse buckling, which is the sum of the y and z components, was then found to be

$$B_t^2 = B_y^2 + B_z^2 = 0.00216 \text{ cm}^{-2} .$$

Figure 3 shows the one-dimensional representation of the UTR-10 which was used for this analysis. The oscillator positions, which correspond to possible access points in the UTR-10, are as follows: 1) 12 cm from the south core tank in the south reflector, 2) in the center of the south core tank, and 3) in the center of the coupling region. The detector locations are positioned in all models used in this study so that A and E are 20 cm from the south and north core tanks respectively and B, C, and D are located in the center of the south core tank, coupling region, and north core tank respectively.

Table 2[1] contains the critical, two-group, nuclear parameters for this model of the UTR-10.

B. Derivation of Green's Function Solution

Under the assumptions that the reactor is operating initially in a steady-state condition at a very low power so that there are no feedback effects and that a localized,

---

[1]Danofsky, R. A., Ames, Iowa. Results of reactor analysis. Private communication. 1969.

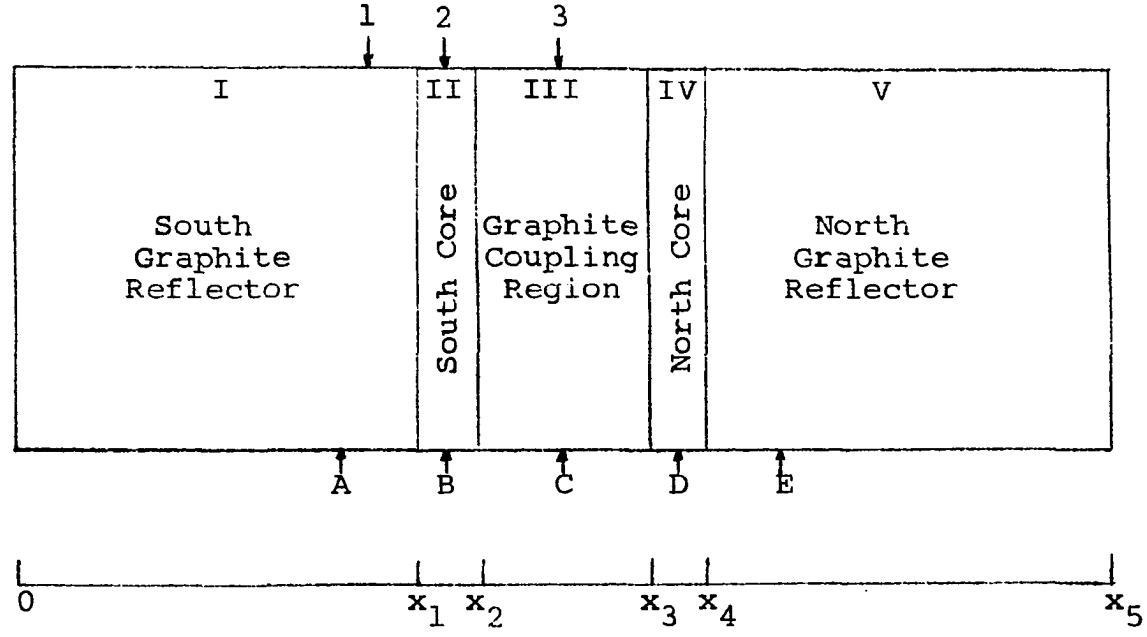

1,2,3 ~ Oscillator Positions
A-E ~ Detector Positions

x_1 = 105 cm
x_2 = 120 cm
x_3 = 165 cm
x_4 = 180 cm
x_5 = 285 cm

Figure 3. Schematic diagram of UTR-10 reactor

Table 2. UTR-10 reactor parameters

Reactor parameter	Region				
	south reflector	south core	coupling region	north core	north reflector
D_F(cm)	1.016	1.23	1.016	1.23	1.016
D_S(cm)	0.840	0.1894	0.840	0.1894	0.840
Σ_r(cm^{-1})	0.00276	0.0267	0.00276	0.0267	0.00276
Σ_a(cm^{-1})	0.00024	0.09079447	0.00024	0.09079447	0.00024
$\nu\Sigma_{fis}$(cm^{-1})	0.0	0.122	0.0	0.122	0.0
v_F(cm/sec)	4.4×10^8				
v_S(cm/sec)	2.2×10^5				
β	0.0064				
λ (sec^{-1})	0.08				

sinusoidal perturbation in the absorption cross section is introduced into one core, Equations B.20 - B.23 of Appendix B are obtained. This case corresponds to having the oscillator at position 2.

Thus, to solve for the flux changes in the north core

$$[|\Delta\tilde{\Sigma}_{af}|\phi_{Sof}\delta(x-x') = 0 \quad \text{since} \quad x \neq x'] \ ,$$

the relevant equations are

$$\frac{d^2}{dx^2}\Delta\hat{\phi}_{Ff} - K_{Ff}^2\Delta\hat{\phi}_{Ff} + H_1\Delta\hat{\phi}_{Sf} = 0 \qquad (23)$$

$$\frac{d^2}{dx^2}\Delta\hat{\phi}_{Sf} - K_{Sf}^2\Delta\hat{\phi}_{Sf} + H_2\Delta\hat{\phi}_{Ff} = 0 \ , \qquad (24)$$

where

$$K_{Ff}^2 = \frac{1}{D_{Ff}}(\Sigma_{rfe} + \frac{j\omega}{v_F}) \ ,$$

$$K_{Sf}^2 = \frac{1}{D_{Sf}}(\Sigma_{afe} + \frac{j\omega}{v_S}) \ ,$$

$$H_1 = \frac{1}{D_{Ff}}[\nu\Sigma_{fis}(1-\beta) + \frac{\lambda\beta\nu\Sigma_{fis}}{\lambda + j\omega}] \ ,$$

and

$$H_2 = \frac{\Sigma_{rf}}{D_{Sf}}$$

(See Appendix B for further definitions.) Equations 23 and 24 form a simultaneous set of differential equations which can be solved by ordinary techniques (41) as shown below.

Thus, solutions of the form

$$\Delta\hat{\phi}_{Ff} = Ae^{\alpha x} \qquad (25a)$$

$$\Delta\hat{\phi}_{Sf} = A'e^{\alpha x} \qquad (25b)$$

are assumed. Substituting Equations 25 into Equations 23 and 24 and dividing out the common factor $e^{\alpha x}$ leads to the

following set of algebraic equations:

$$(\alpha^2 - K_{Ff}^2)A + H_1 A' = 0 \tag{26}$$

$$H_2 A + (\alpha^2 - K_{Sf}^2)A' = 0 \quad . \tag{27}$$

Non-trivial solutions for A and A' will exist only if the determinant of the coefficients of Equations 26 and 27 is zero; that is,

$$\begin{vmatrix} \alpha^2 - K_{Ff}^2 & H_1 \\ H_2 & \alpha^2 - K_{Sf}^2 \end{vmatrix} = \alpha^4 - (K_{Ff}^2 + K_{Sf}^2)\alpha^2 + K_{Ff}^2 K_{Sf}^2 - H_1 H_2 = 0 \quad .$$

Therefore,

$$\alpha^2 = 1/2[(K_{Ff}^2 + K_{Sf}^2) \pm \sqrt{(K_{Ff}^2 + K_{Sf}^2)^2 - 4(K_{Ff}^2 K_{Sf}^2 - H_1 H_2)}] \quad ,$$

and the four values of α are:

$$\alpha_1 = [1/2(K_{Ff}^2 + K_{Sf}^2) + 1/2\sqrt{(K_{Ff}^2 + K_{Sf}^2)^2 - 4(K_{Ff}^2 K_{Sf}^2 - H_1 H_2)}]^{1/2} \tag{28}$$

$$\alpha_2 = -\alpha_1 \tag{29}$$

$$\alpha_3 = [1/2(K_{Ff}^2 + K_{Sf}^2) - 1/2\sqrt{(K_{Ff}^2 + K_{Sf}^2)^2 - 4(K_{Ff}^2 K_{Sf}^2 - H_1 H_2)}]^{1/2} \tag{30}$$

$$\alpha_4 = -\alpha_3 \tag{31}$$

Thus, the solutions, Equations 25, become

$$\hat{\Delta\phi}_{Ff} = A_1 e^{\alpha_1 x} + A_2 e^{\alpha_2 x} + A_3 e^{\alpha_3 x} + A_4 e^{\alpha_4 x} \tag{32a}$$

$$\hat{\Delta\phi}_{Sf} = A_1' e^{\alpha_1 x} + A_2' e^{\alpha_2 x} + A_3' e^{\alpha_3 x} + A_4' e^{\alpha_4 x} \quad . \tag{32b}$$

It may be shown that only four of the eight constants in Equations 32 are independent.

Equations 32 are the complete and most general solutions of Equations 23 and 24, but permissible solutions are also $\hat{\Delta\phi}_{Ff} = A_1 e^{\alpha_1 x}$ and $\hat{\Delta\phi}_{Sf} = A_1' e^{\alpha_1 x}$. Substituting these into Equation 23 (or Equation 24) and dividing out $e^{\alpha_1 x}$ yields

$$(\alpha_1^2 - K_{Ff}^2) A_1 + H_1 A_1' = 0 \quad .$$

Defining a coupling coefficient

$$S_1 = \frac{A_1'}{A_1} \quad ,$$

then

$$S_1 = \frac{K_{Ff}^2 - \alpha_1^2}{H_1} \quad ,$$

and similarly

$$S_i = \frac{K_{Ff}^2 - \alpha_i^2}{H_1} \quad , \quad i = 1,2,3,4. \tag{33}$$

The coupling coefficients are not arbitrary since they depend on the reactor parameters. Therefore, the solutions, Equations 32, become

$$\Delta\hat{\phi}_{Ff} = A_1 e^{\alpha_1 x} + A_2 e^{\alpha_2 x} + A_3 e^{\alpha_3 x} + A_4 e^{\alpha_4 x} \qquad (34a)$$

$$\Delta\hat{\phi}_{Sf} = S_1 A_1 e^{\alpha_1 x} + S_2 A_2 e^{\alpha_2 x} + S_3 A_3 e^{\alpha_3 x} + S_4 A_4 e^{\alpha_4 x} . \qquad (34b)$$

It can be noted in passing that inspection of Equation 33 reveals that $S_1 = S_2$ and $S_3 = S_4$.

To solve for the flux changes in the graphite moderator regions, the relevant equations are (from Appendix B)

$$\frac{d^2}{dx^2}\Delta\hat{\phi}_{Fm} - K_{Fm}^2\Delta\hat{\phi}_{Fm} = 0 \qquad (35)$$

$$\frac{d^2}{dx^2}\Delta\hat{\phi}_{Sm} - K_{Sm}^2\Delta\hat{\phi}_{Sm} + H_3\Delta\hat{\phi}_{Fm} = 0 , \qquad (36)$$

where

$$K_{Fm}^2 = \frac{1}{D_{Fm}}(\Sigma_{rme} + \frac{j\omega}{v_F}) ,$$

$$K_{Sm}^2 = \frac{1}{D_{Sm}}(\Sigma_{ame} + \frac{j\omega}{v_S}) ,$$

and

$$H_3 = \frac{\Sigma_{rm}}{D_{Sm}} .$$

Equation 35 can be solved directly using the method of Glasstone and Edlund (19). Thus,

$$\Delta\hat{\phi}_{Fm} = E_1 e^{K_{Fm}x} + E_2 e^{-K_{Fm}x} \quad . \tag{37}$$

The solution for the homogeneous part (first two terms) of Equation 36 has the same form as Equation 37, and thus, the general solution to Equation 36 is

$$\Delta\hat{\phi}_{Sm} = E_3 e^{K_{Sm}x} + E_4 e^{-K_{Sm}x} + S_5\Delta\hat{\phi}_{Fm} \quad , \tag{38}$$

where S_5 is a coupling coefficient. S_5 can be evaluated using a procedure similar to that used to evaluate $S_1 - S_4$ as is shown below.

Equation 38 is the complete and most general solution to Equation 36, but a permissible solution is $\Delta\hat{\phi}_{Sm} = S_5\Delta\hat{\phi}_{Fm}$. Substituting this into Equation 36 yields

$$S_5\frac{d^2}{dx^2}\Delta\hat{\phi}_{Fm} - K_{Sm}^2 S_5\Delta\hat{\phi}_{Fm} + H_3\Delta\hat{\phi}_{Fm} = 0 \quad . \tag{39}$$

By Equation 35,

$$\frac{d^2}{dx^2}\Delta\hat{\phi}_{Fm} = K_{Fm}^2\Delta\hat{\phi}_{Fm} \quad ;$$

therefore Equation 39 becomes

$$S_5 K_{Fm}^2\Delta\hat{\phi}_{Fm} - S_5 K_{Sm}^2\Delta\hat{\phi}_{Fm} + H_3\Delta\hat{\phi}_{Fm} = 0 \quad .$$

Thus,

$$S_5 = \frac{H_3}{K_{Sm}^2 - K_{Fm}^2} \quad . \tag{40}$$

S_5 depends on the reactor parameters, so it is not arbitrary.

The solutions in all three moderator regions have the same form as Equations 37 and 38, but they are not identical. To account for their differences, the solutions for these three regions can be written as follows:

Solutions for south reflector:

$$\Delta\hat{\phi}_{Fm} = E_1 e^{K_{Fm}x} + E_2 e^{-K_{Fm}x} \tag{41a}$$

$$\Delta\hat{\phi}_{Sm} = S_5 E_1 e^{K_{Fm}x} + S_5 E_2 e^{-K_{Fm}x} + E_3 e^{K_{Sm}x} + E_4 e^{-K_{Sm}x} \quad . \tag{41b}$$

Solutions for coupling region:

$$\Delta\hat{\phi}_{Fm} = C_1 e^{K_{Fm}x} + C_2 e^{-K_{Fm}x} \tag{42a}$$

$$\Delta\hat{\phi}_{Sm} = S_5 C_1 e^{K_{Fm}x} + S_5 C_2 e^{-K_{Fm}x} + C_3 e^{K_{Sm}x} + C_4 e^{-K_{Sm}x} \quad . \tag{42b}$$

Solutions for north reflector:

$$\Delta\hat{\phi}_{Fm} = F_1 e^{K_{Fm}x} + F_2 e^{-K_{Fm}x} \tag{43a}$$

$$\Delta\hat{\phi}_{Sm} = S_5 F_1 e^{K_{Fm}x} + S_5 F_2 e^{-K_{Fm}x} + F_3 e^{K_{Sm}x} + F_4 e^{-K_{Sm}x} \quad . \tag{43b}$$

To solve for the flux changes in the south core, the relevant equations are (from Appendix B)

$$\frac{d^2}{dx^2}\Delta\hat{\phi}_{Ff} - K_{Ff}\Delta\hat{\phi}_{Ff} + H_1\Delta\hat{\phi}_{Sf} = 0 \tag{44}$$

$$\frac{d^2}{dx^2}\Delta\hat{\phi}_{Sf} - K_{Sf}\Delta\hat{\phi}_{Sf} + H_2\Delta\hat{\phi}_{Ff} + \frac{|\Delta\bar{\Sigma}_{af}|\phi_{Sof}}{D_{Sf}}\delta(x-x') = 0 \; . \tag{45}$$

K_{Ff}, K_{Sf}, H_1, and H_2 have the same meanings here as they do in Equations 23 and 24. The values of $|\Delta\bar{\Sigma}_{af}|$ and ϕ_{Sof} are arbitrary (providing $|\Delta\bar{\Sigma}_{af}|$ is small); therefore they can be adjusted so that

$$\frac{|\Delta\bar{\Sigma}_{af}|\phi_{Sof}}{D_{Sf}} = 1 \; .$$

Thus, Equations 44 and 45 can be rewritten as

$$\begin{bmatrix} \frac{d^2}{dx^2} - K_{Ff}^2 & H_1 \\ H_2 & \frac{d^2}{dx^2} - K_{Sf}^2 \end{bmatrix} \begin{bmatrix} \Delta\hat{\phi}_{Ff} \\ \Delta\hat{\phi}_{Sf} \end{bmatrix} + \begin{bmatrix} 0 \\ \delta(x-x') \end{bmatrix} = \begin{bmatrix} 0 \\ 0 \end{bmatrix} \; . \tag{46}$$

Equation 46 has the same form as Equation 1 with

$$L = \begin{bmatrix} \frac{d^2}{dx^2} - K_{Ff}^2 & H_1 \\ H_2 & \frac{d^2}{dx^2} - K_{Sf}^2 \end{bmatrix} \; ,$$

$$Y = \begin{bmatrix} \hat{\Delta\phi}_{Ff} \\ \hat{\Delta\phi}_{Sf} \end{bmatrix} ,$$

and

$$\Phi = \begin{bmatrix} 0 \\ \delta(x-x') \end{bmatrix} .$$

Thus, it should be possible to obtain a Green's function solution to Equation 46, and since Φ is a delta function, the solution should have the same form as Equation 9; that is, $\hat{\Delta\phi}_{Ff} = G_F$ and $\hat{\Delta\phi}_{Sf} = G_S$.

Proceeding in a manner analogous to the solution of the slab reactor, the first condition on the Green's function requires

$$\begin{bmatrix} \frac{d^2}{dx^2} - K_{Ff}^2 & H_1 \\ H_2 & \frac{d^2}{dx^2} - K_{Sf}^2 \end{bmatrix} \begin{bmatrix} G_F \\ G_S \end{bmatrix} = \begin{bmatrix} 0 \\ 0 \end{bmatrix} . \qquad (47)$$

Equation 47 is identical to the set, Equations 23 and 24; therefore the solutions will have the same form as Equations 34. Thus, for $x < x'$

$$G_{F1} = \hat{\Delta\phi}_{Ff} = U_1 e^{\alpha_1 x} + U_2 e^{\alpha_2 x} + U_3 e^{\alpha_3 x} + U_4 e^{\alpha_4 x} \qquad (48a)$$

$$G_{S1} = \hat{\Delta\phi}_{Sf} = S_1U_1e^{\alpha_1 x} + S_2U_2e^{\alpha_2 x} + S_3U_3e^{\alpha_3 x} + S_4U_4e^{\alpha_4 x} \quad , \tag{48b}$$

and for $x > x'$

$$G_{F2} = \hat{\Delta\phi}_{Ff} = V_1e^{\alpha_1 x} + V_2e^{\alpha_2 x} + V_3e^{\alpha_3 x} + V_4e^{\alpha_4 x} \tag{49a}$$

$$G_{S2} = \hat{\Delta\phi}_{Sf} = S_1V_1e^{\alpha_1 x} + S_2V_2e^{\alpha_2 x} + S_3V_3e^{\alpha_3 x} + S_4V_4e^{\alpha_4 x} \quad . \tag{49b}$$

The continuity conditions on the fluxes and currents at the various region interfaces have the effect of continuing the left and right hand parts of the Green's function out to the reactor boundaries, which allows the second condition on the Green's function to be fulfilled. For example, going from the south core to the south reflector and then to the south boundary yields the following relationships:

At $x = x_1$ (see Figure 3)

$$\hat{\Delta\phi}_{Fm}(I) = \hat{\Delta\phi}_{Ff}(II)$$

or

$$E_1e^{K_{Fm}x_1} + E_2e^{-K_{Fm}x_1} = U_1e^{\alpha_1 x_1} + U_2e^{\alpha_2 x_1} + U_3e^{\alpha_3 x_1} + U_4e^{\alpha_4 x_1}$$

and

$$D_{Fm}\frac{d\hat{\Delta\phi}_{Fm}(I)}{dx} = D_{Ff}\frac{d\hat{\Delta\phi}_{Ff}(II)}{dx}$$

or

$$D_{Fm}E_1K_{Fm}e^{K_{Fm}x_1} - D_{Fm}E_2K_{Fm}e^{-K_{Fm}x_1} = D_{Ff}U_1\alpha_1 e^{\alpha_1 x_1}$$

$$+ D_{Ff}U_2\alpha_2 e^{\alpha_2 x_1} + D_{Ff}U_3\alpha_3 e^{\alpha_3 x_1} + D_{Ff}U_4\alpha_4 e^{\alpha_4 x_1} \quad .$$

Similar expressions hold for $\hat{\Delta\phi}_{Sm}(I)$ and $\hat{\Delta\phi}_{Sf}(II)$.

At $x = 0$,

$$\hat{\Delta\phi}_{Fm}(I) = 0$$

or

$$E_1 e^{K_{Fm}(o)} + E_2 e^{-K_{Fm}(o)} = E_1 + E_2 = 0 \quad .$$

A similar expression holds for $\hat{\Delta\phi}_{Sm}(I)$. Analogous expressions hold at the region interfaces in going in succession from the south core to the coupling region to the north core to the north reflector to the north boundary. Thus, the second condition on the Green's function is fulfilled; since in the south reflector, the Green's function is represented by $\hat{\Delta\phi}_{Fm}(I)$ and $\hat{\Delta\phi}_{Sm}(I)$ which go to zero at $x = 0$ and in the north reflector, the Green's function is represented by $\hat{\Delta\phi}_{Fm}(V)$ and $\hat{\Delta\phi}_{Sm}(V)$ which go to zero at $x = x_5 = 285$cm.

The third condition on the Green's function requires that at $x = x'$ (oscillator position 2)

$$G_{F1}(x') = G_{F2}(x')$$

and

$$G_{S1}(x') = G_{S2}(x') \quad .$$

The fourth condition on the Green's function requires that at $x = x'$

$$\frac{dG_{F2}(x')}{dx} - \frac{dG_{F1}(x')}{dx} = 0$$

and

$$\frac{dG_{S2}(x')}{dx} - \frac{dG_{S1}(x')}{dx} = -1 \quad .$$

These relationships are based on the intuition that the fast flux should not have a discontinuity in its first derivative from a perturbation in the slow absorption cross section, and this is proven to be correct in Appendix C which shows that this formulation is equivalent to the Green's function solution of the fourth-order differential equation resulting from the combination of the two-group diffusion equations.

Thus, in the set of solutions for the flux changes in the five regions of the reactor (Equations 34, 41, 42, 43, 48, and 49), there are 24 independent and undetermined constants, but there are also 24 conditions (Green's function and continuity conditions) available to solve for them. Therefore, each of these constants may be determined uniquely, so that the solutions can be obtained for any point in the reactor.

Analogous to the case of the slab reactor, the solutions $\hat{\Delta\phi}_F$ and $\hat{\Delta\phi}_S$ are complex; therefore they can be written as

$$\hat{\Delta\phi}_F = a_1 + jb_1$$

$$\hat{\Delta\phi}_S = a_2 + jb_2 \quad .$$

Thus, the magnitude of the response in decibels is

$$\text{Fast Mag.} = 20 \log_{10}\sqrt{a_1^2 + b_1^2} \tag{50}$$

$$\text{Slow Mag.} = 20 \log_{10}\sqrt{a_2^2 + b_2^2} \quad , \tag{51}$$

and the phase angle in degrees is

$$\text{Fast Phase} = \frac{180}{\pi}\left(\tan^{-1}\frac{b_1}{a_1}\right) \tag{52}$$

$$\text{Slow Phase} = \frac{180}{\pi}\left(\tan^{-1}\frac{b_2}{a_2}\right) \quad . \tag{53}$$

C. Frequency Response Results

The frequency response of the slow group was obtained at detector positions A, D, and E with the oscillator at position 2. The relative magnitude of the response is shown in Figure 4 and the phase in Figure 5. Also plotted in these figures are the results obtained by Merritt (35) for this same

case, using the Green's function mode approximation. Merritt has normalized his results (both magnitude and phase responses) to single curves at low frequencies. For the results obtained here it was decided to show the spread of the response curves at low frequencies; therefore the only normalization performed here was to set the magnitude response at 10^{-2} rad/sec for detector position A to 0 db.

As in the case of the slab reactor, these results at low frequencies are similar to the space-independent model, as expected. The phase angle approaches -90^{o} at low frequencies and the magnitude response shows a break at λ(0.08 rad/sec) in accordance with the space-independent model.

Danofsky and Uhrig (14) have shown that the break frequencies of the magnitude response of the UTR-10 reactor still occur at λ and β/Λ. Since β/Λ for the UTR-10 is in the 30-60 rad/sec range, the results here are in excellent agreement with that analysis.

In comparing these results with those obtained by Merritt (35), there are several noticeable differences. At low frequencies, the phase angle obtained from the Green's function mode approximation decreases to less than -110^{o} instead of approaching -90^{o}; and at high frequencies, with the possible exception of position D, the phase angles are decreasing steadily. The results obtained here indicate

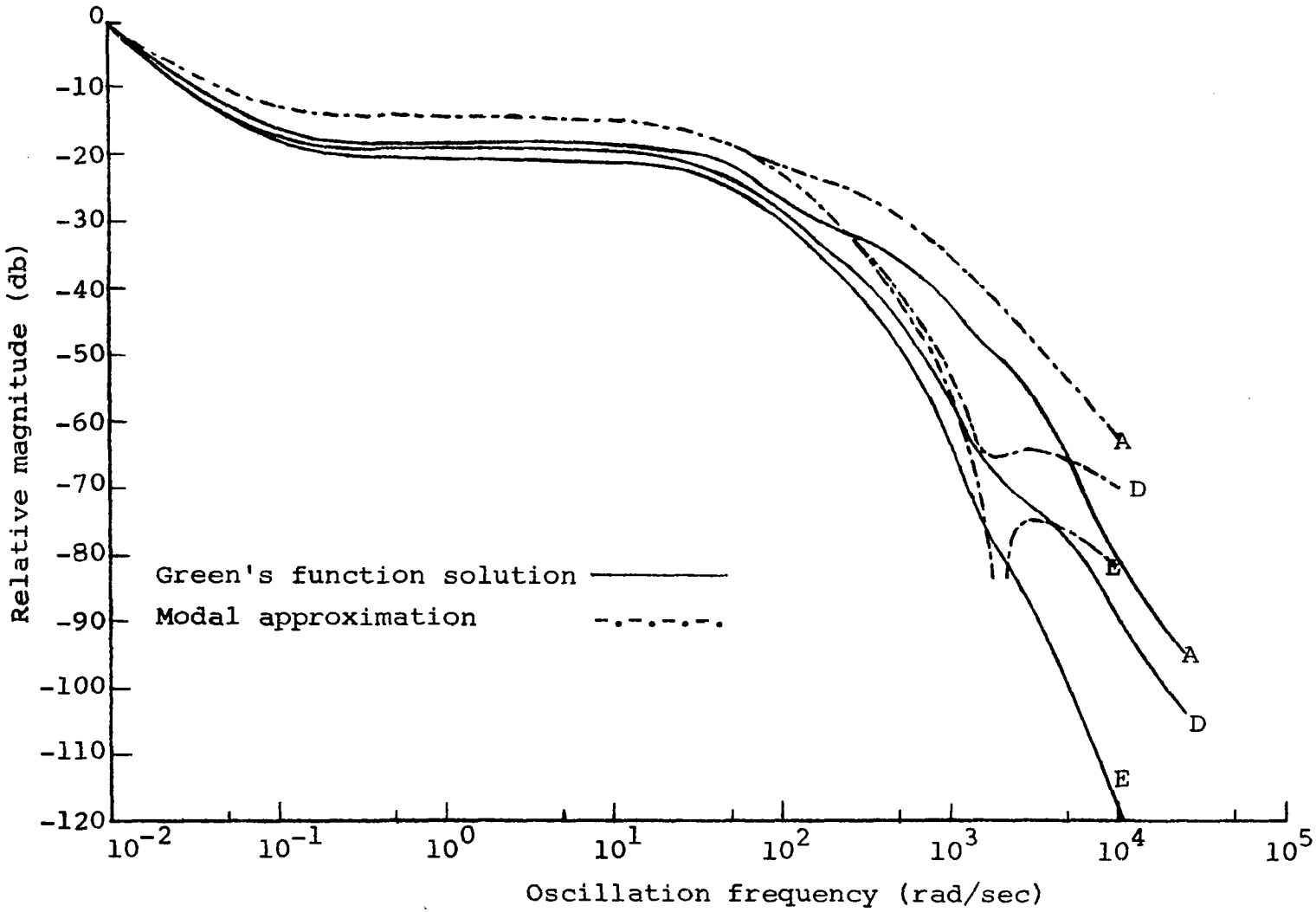

Figure 4. Magnitude of frequency response, oscillator at position 2

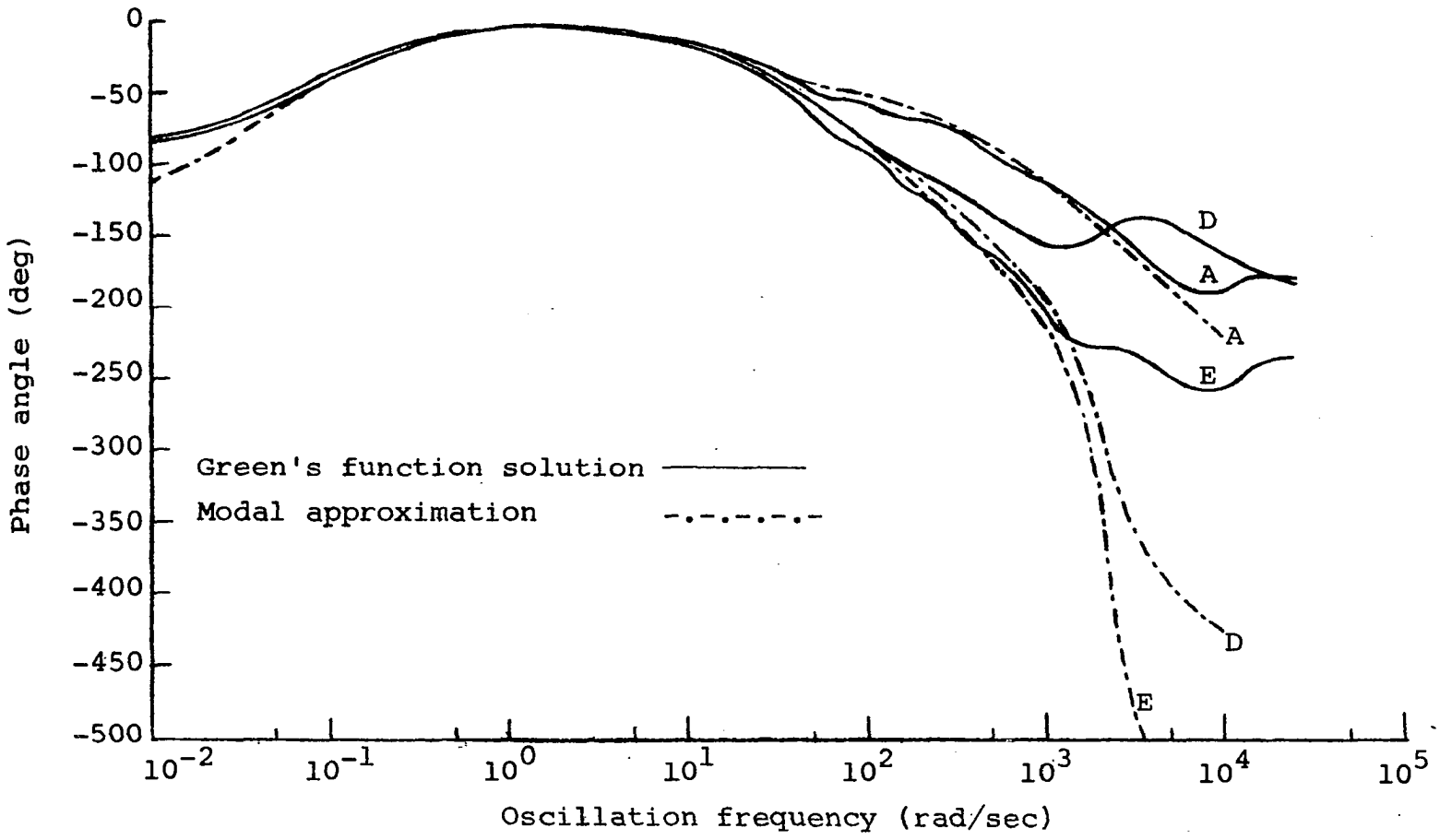

Figure 5. Phase of frequency response, oscillator at position 2

that the phase angles are approaching asymptotic values at high frequencies, which is the expected behavior (35). The results obtained by Betancourt (7) for this case, using the natural mode approximation, do not show as great a phase angle decrease at high frequencies as the Green's function mode approximation, but neither do they show the phase angles approaching asymptotic values.

The magnitude response determined by the Green's function mode approximation shows a sink effect at about 2000 rad/sec at positions D and E, with the sink at position E being more pronounced. The results obtained here at those two positions show inflection points in the response curves at that same frequency, with the inflection at position D being more pronounced. The results obtained by the natural mode approximation do not show a sink or inflection point in the magnitude response curve for position D, but they do show a sink effect at slightly less than 1000 rad/sec in the response at position E. The possibility that the sink phenomenon actually exists is not without precedent, as is pointed out by both Betancourt (7) and Merritt (35), but Betancourt also acknowledges that the modal approximations may have convergence problems at these frequencies.

However, although the three methods are not in good agreement, they all do predict some sort of unexpected behavior; and thus, it is likely that some unexpected

phenomenon is occurring at these frequencies. Merritt (35) has suggested, as a possible explanation, that the fast group perturbation from the south core is thermalized in the north core; and at a frequency of about 2000 rad/sec (calculated from the perturbation transit time from the south core to the north core), is 180^{o} out of phase with the slow group perturbation propagated to the north core. This would have a partial cancellation effect (complete cancellation could occur only if the amplitudes were exactly the same) on the magnitude response and could account for a sink; since as the frequency increased, the thermalized fast group perturbation would become less out of phase with the slow group perturbation, which would have an additive effect on the magnitude response. However, as Merritt (35) has pointed out, the actual formation of a sink would require that the amplitudes of the thermalized fast group perturbation and the slow group perturbation be very nearly the same. If there is a significant difference in these amplitudes, the effect would only be a slight flattening of the magnitude response curve, which is the result predicted in this study.

Although a detailed analysis of the frequency response in this frequency range would be desirable, it is beyond the scope of this work.

V. PARAMETRIC ANALYSIS OF A COUPLED CORE REACTOR

Using the UTR-10 model (as described in Section IV) as a basis, the effects of various parameters on the frequency response of a coupled-core reactor were investigated with the Green's function solution technique developed in Section IV. The parameters chosen for study were 1) oscillator and detector position, 2) the effect of neglecting delayed neutrons and considering $1/v_f$ to be negligibly small, 3) neutron energy group, 4) neutron group speeds, 5) the delayed neutron fraction β, and 6) coupling region width. These parameters were chosen because it was felt that their effects might be important. Merritt (35) has investigated the effects of some of these parameters using the Green's function mode approximation, and where possible, comparisons will be made between his results and those obtained here.

A. Effect of Oscillator and Detector Position

In the UTR-10 reactor there are three potential oscillator positions of particular interest, as shown in Figure 3. As noted before, these positions are 1) 12 cm from the south core tank in the south reflector, 2) in the center of a core tank (the south core tank was used), and 3) in the center of the coupling region.

The spatial dependence of the frequency response was investigated by determining the response at the five detector

locations A-E shown in Figure 3. As noted before, A is 20 cm from the south core tank in the south reflector, E is 20 cm from the north core tank in the north reflector, and B, C, and D are in the center of the south core tank, coupling region, and north core tank respectively.

Figures 6-11 show the magnitude and phase of the frequency response at detector positions A-E with the oscillator at positions 1-3. Inspection of these figures reveals that in all cases the response at frequencies below ~ 10 rad/sec is nearly identical with that of the space-independent model. Also noticeable for all cases is the resonance effect in the magnitude and phase when the oscillator and detector are located at or near the same point. This effect has also been found in conventional reactors (20). Inspection of the magnitude response curves also shows that at positions far from the oscillator the value of the β/Λ frequency break is more consistent (~ 50 rad/sec) and greater than at positions close to the oscillator. This behavior has also been noted in the analysis of conventional reactors (34).

With the oscillator at position 1, the magnitude response curves at detector positions D and E show the same type of inflection points at the same frequency (~ 2000 rad/sec) as do these two curves when the oscillator is at position 2. The phase angle curves for these two cases also show inflection points or actual phase reversals at this

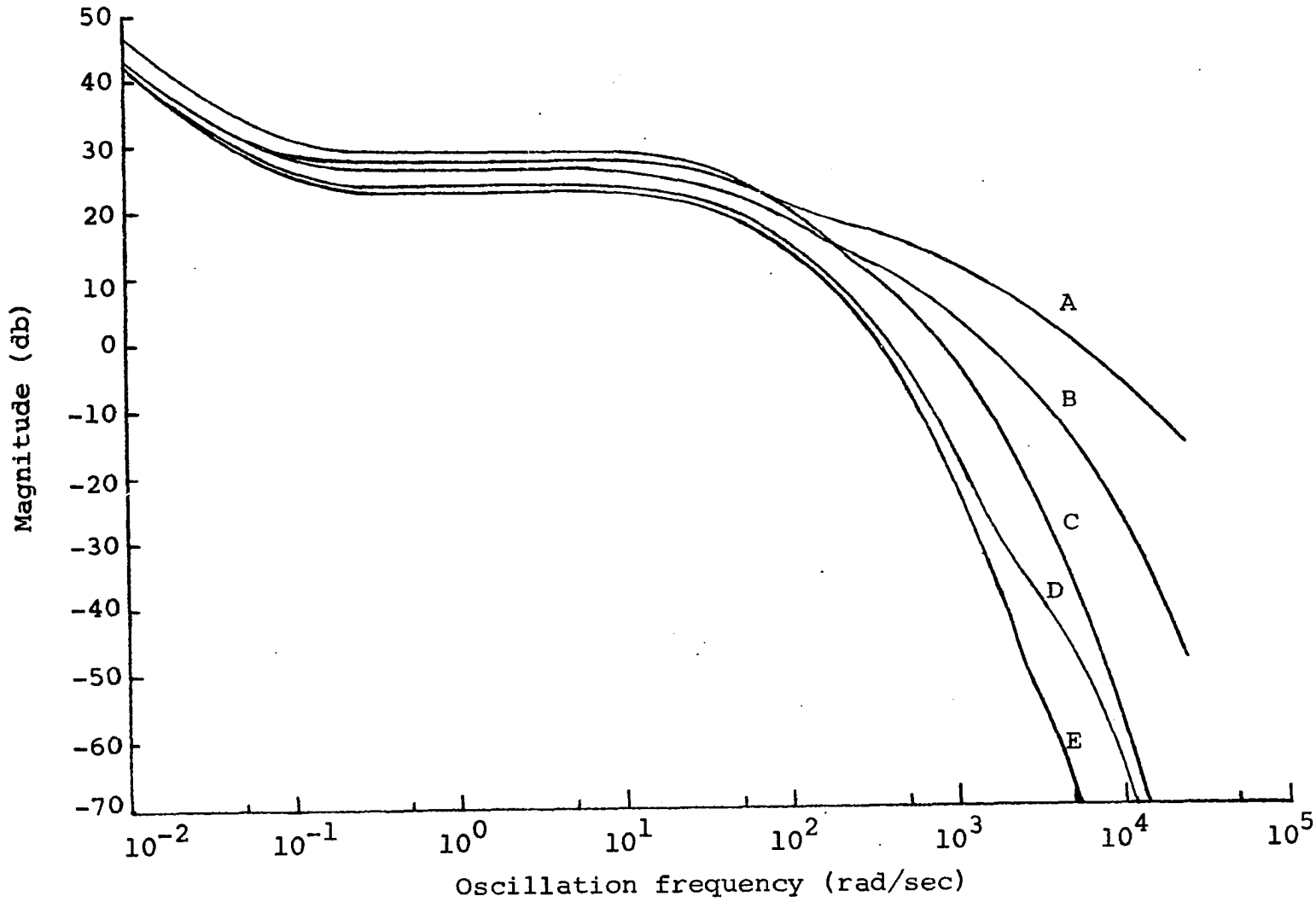

Figure 6. Magnitude of frequency response, oscillator at position 1

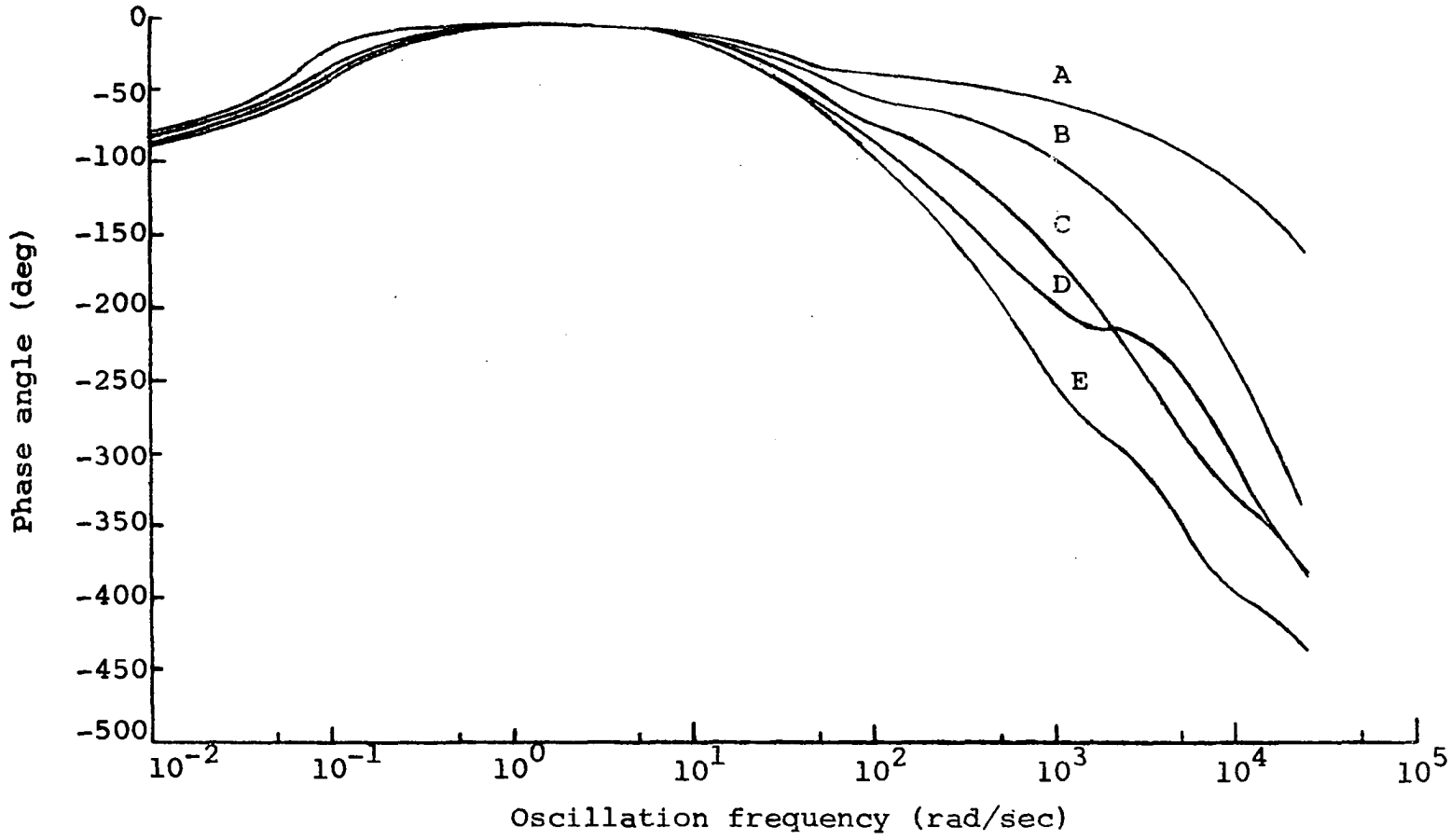

Figure 7. Phase of frequency response, oscillator at position 1

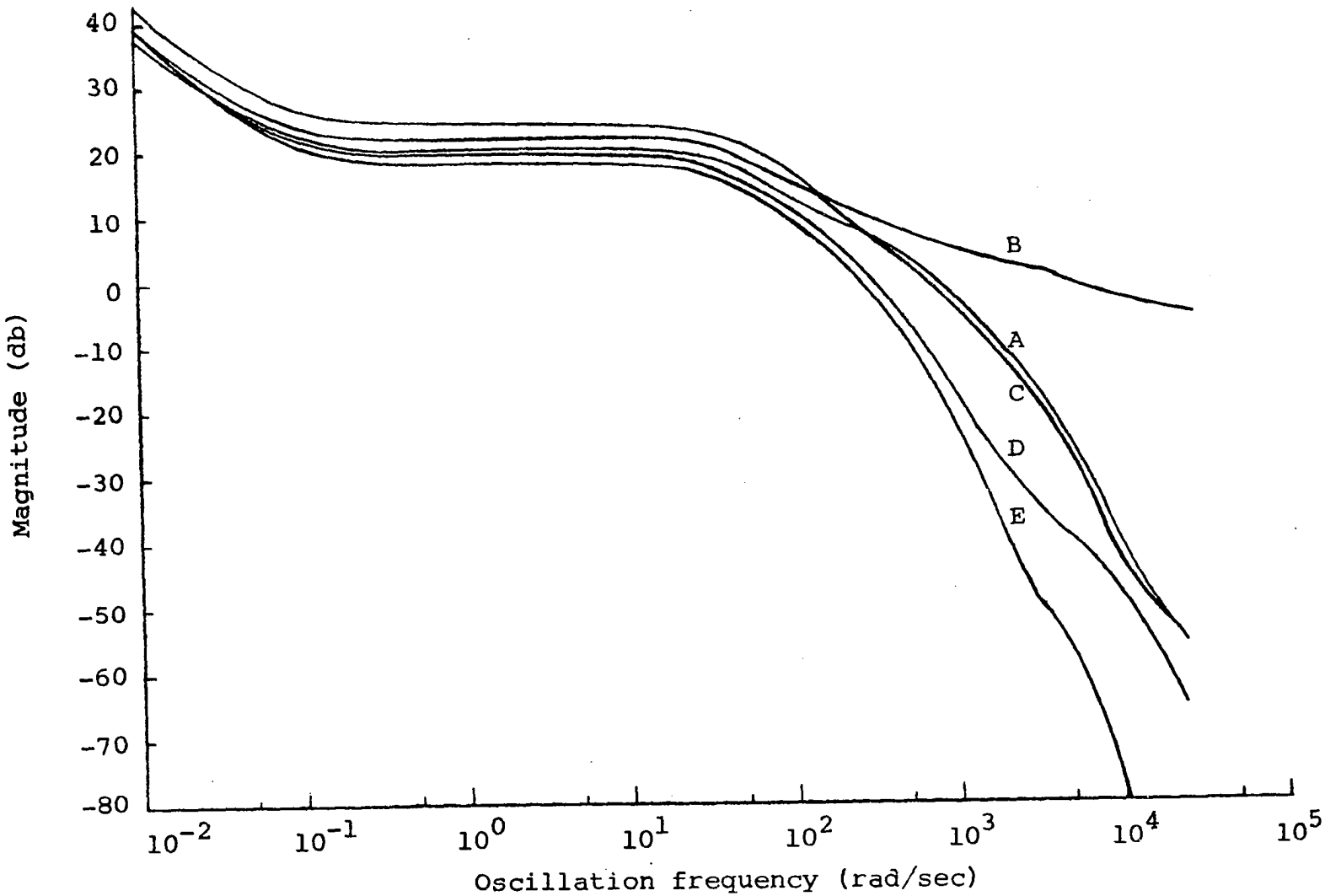

Figure 8. Magnitude of frequency response, oscillator at position 2

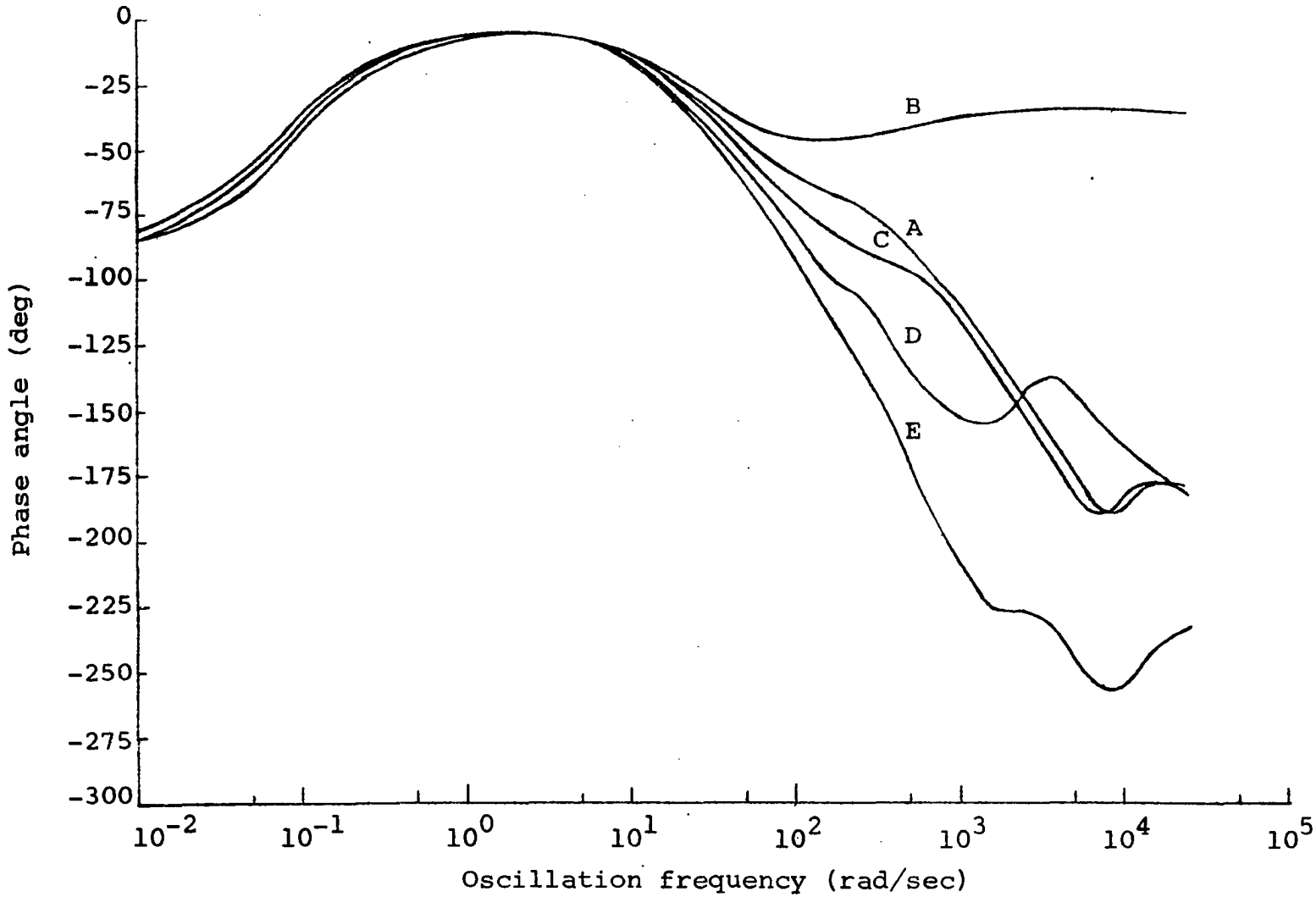

Figure 9. Phase of frequency response, oscillator at position 2

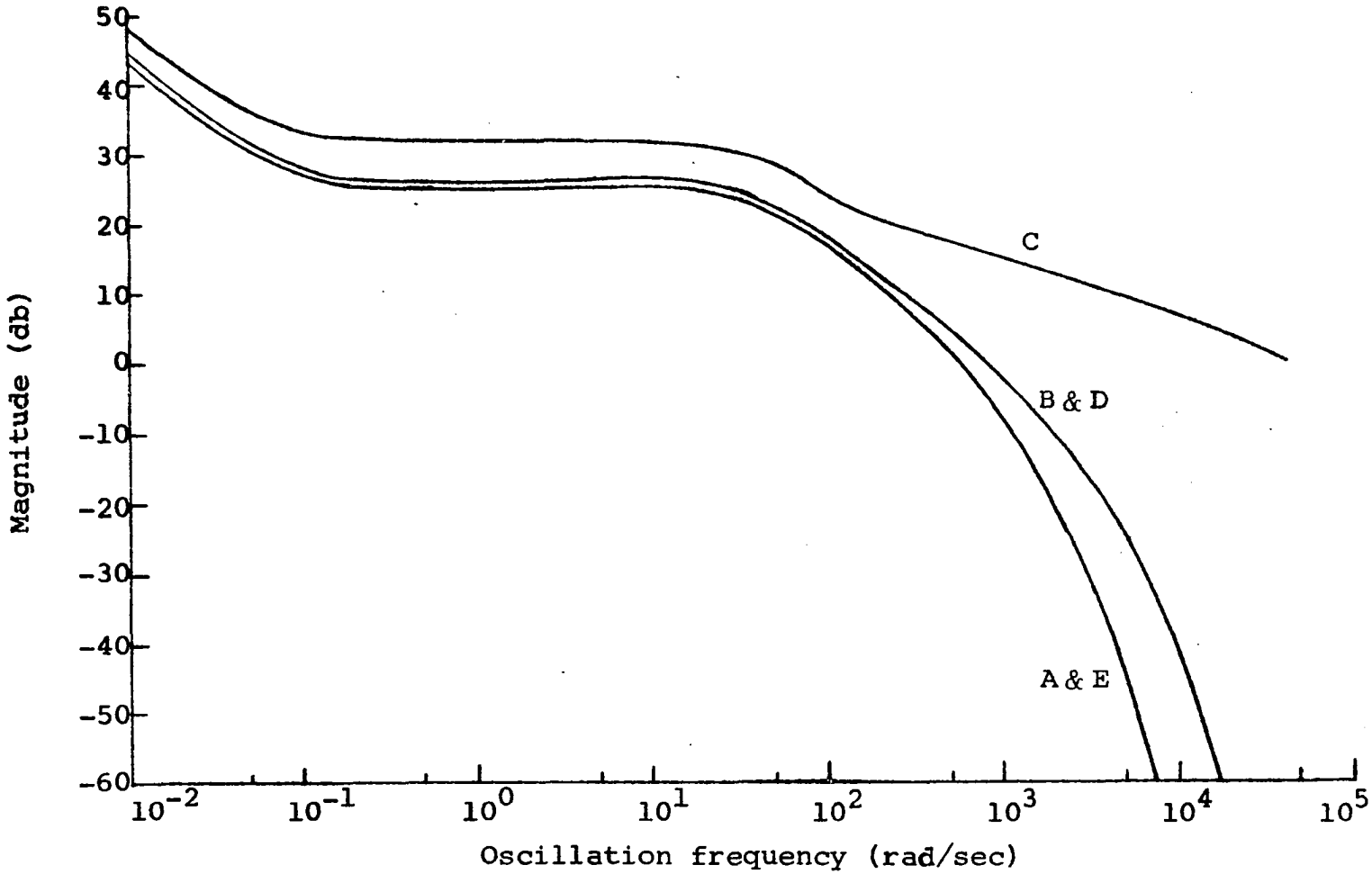

Figure 10. Magnitude of frequency response, oscillator at position 3

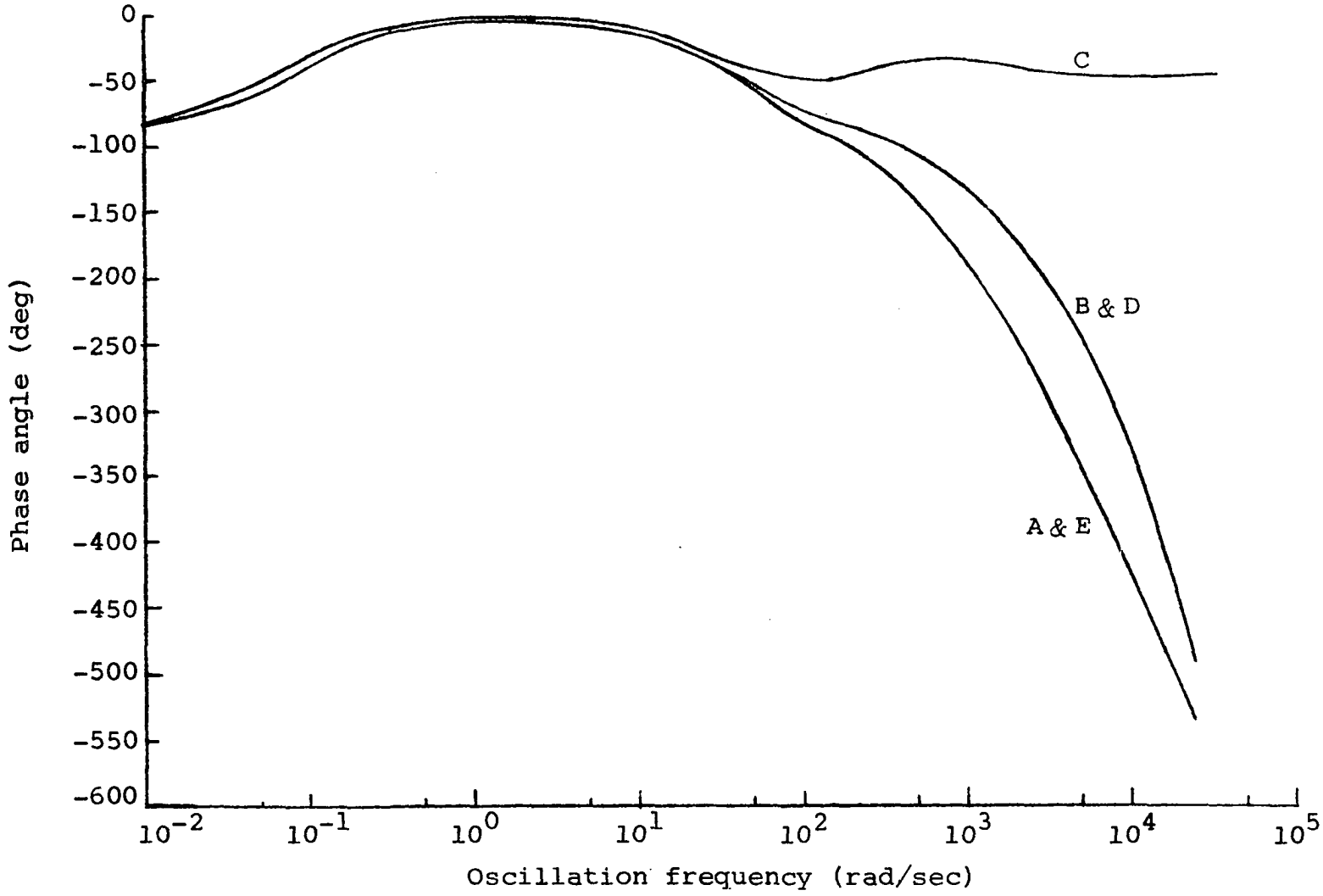

Figure 11. Phase of frequency response, oscillator at position 3

same frequency. It is reasonable that this behavior should also occur with the oscillator at position 2; since at both locations, the response at D and E is the result of the perturbation propagating through the south core, coupling region, and north core. That this behavior occurs only at D and E indicates that the cause is some kind of interaction phenomenon between the two cores. The results obtained by Merritt (35) at these two oscillator positions are in good agreement with the results obtained here at detector positions A, B, and C. However, at positions D and E with the oscillator at position 1, Merritt's results for the magnitude and phase show no unusual behavior. Merritt's results at D and E with the oscillator at position 2 are shown in Figures 4 and 5, and the outstanding feature of those curves is the sink in the magnitude response at 2000 rad/sec.

With the oscillator at position 3, the responses are similar to those of two identical, reflected slab reactors; since both cores are being perturbed equally instead of, as in the previous cases, one core being driven by the other. The results obtained by Merritt (35) for this case show the same type of behavior as the results obtained here.

B. Effect of Neglecting Delayed Neutrons and Considering $1/v_F$ to be Negligibly Small

The approximations of neglecting delayed neutrons and considering $1/v_F$ to be zero were chosen for study, because at the frequency (~ 2000 rad/sec) at which the inflection points occur in the response curves for detector positions D and E, the effect of these parameters should be negligible. The effect of these assumptions on the UTR-10 model is to change Equation 23 so that

$$K_{Ff}^2 = \frac{\Sigma_{rfe}}{D_{Ff}} \qquad \text{and} \qquad H_1 = \frac{\nu\Sigma_{fis}}{D_{Ff}} \quad .$$

With these changes, the frequency response above 10 rad/sec was the same as before.

Thus, these parameters can definitely be eliminated as possible causes of the unusual behavior in the response noted above. Also, this shows that the UTR-10 model is giving results which are consistent with the expected behavior.

C. Dependence on Neutron Energy Groups

With the model being used in this study, the dependence of the frequency response on the neutron energy group can be checked for only the fast and slow groups. Figures 12 and 13 show the magnitude and phase of the fast group frequency response at the five detector positions A-E with the

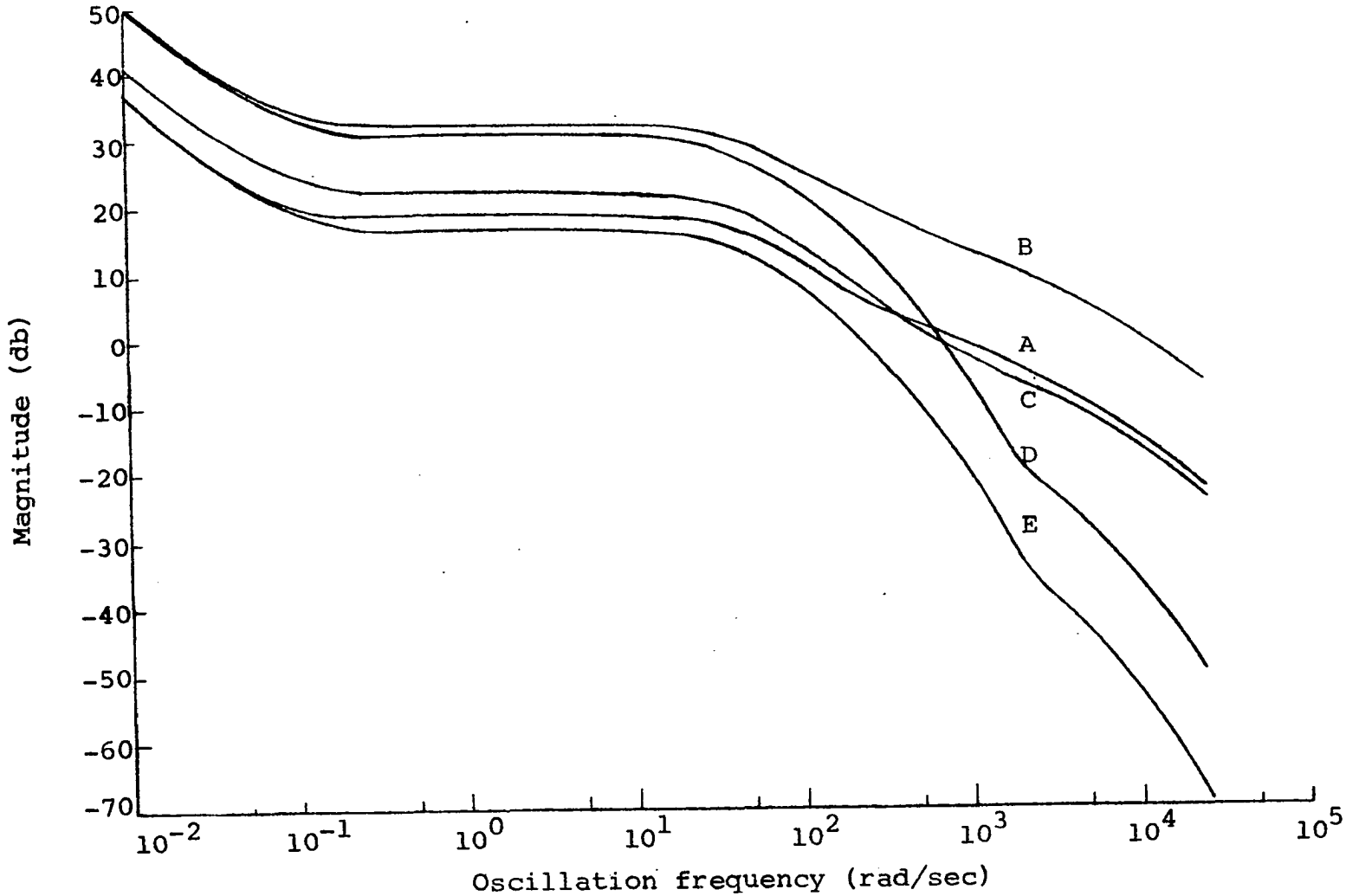

Figure 12. Magnitude of frequency response for fast group, oscillator at position 2

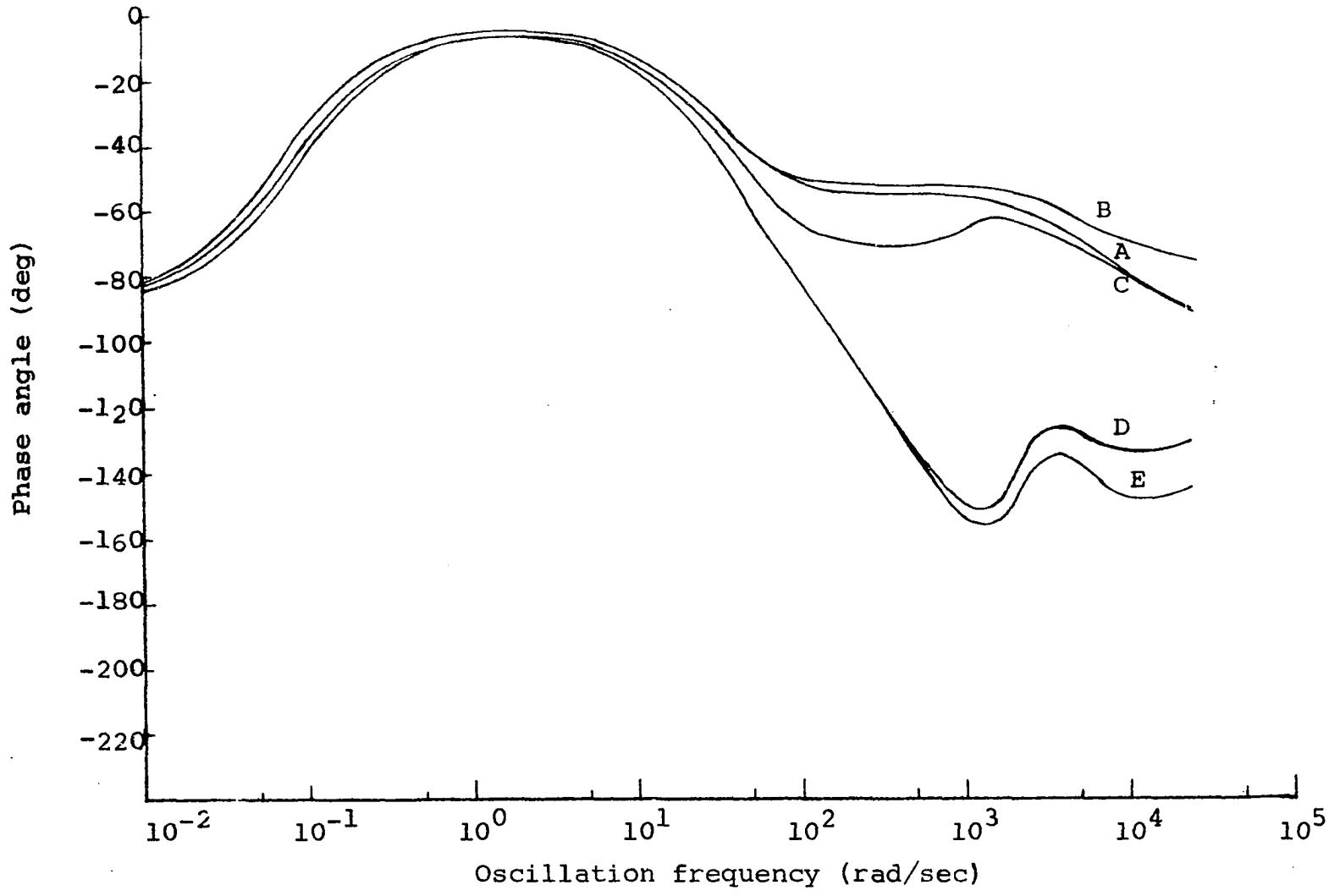

Figure 13. Phase of frequency response for fast group, oscillator at position 2

oscillator at position 2. Figures 8 and 9 show the corresponding slow group responses.

In comparing the fast and slow group responses at each detector position, it can be seen that at low frequencies the responses are generally the same, and at high frequencies the fast group tends to show a greater magnitude response and less phase shift than the slow group. A similar effect was found by Merritt (35), and as he pointed out, it is caused by the fast group's larger velocity and correspondingly greater attenuation length.

The fast group magnitude response curves for detector positions D and E show the same kind of inflection at ~ 2000 rad/sec as do the slow group curves. The fast group phase curves for these positions also show phase reversals at this frequency. This behavior is not surprising since the fast group response at these positions is caused by the oscillations of the slow group in the north core. This is so because the fast group oscillations from the south core are completely thermalized by the time they reach these positions.

D. Dependence on Neutron Group Speeds

The dependence of the frequency response on the neutron group speeds was determined to make possible another comparison between results obtained here and those obtained by

Merritt (35) using the Green's function mode approximation.

The comparison value of v_F used here and by Merritt (35) was 3.0×10^6 cm/sec. With this value of v_F there was practically no difference in the frequency response at low frequencies. At high frequencies, especially at detector positions far from the oscillator, the use of this value of v_F resulted in larger phase shifts. Merritt (35) obtained these same results with this value of v_F.

The comparison value of v_S used here and by Merritt (35) was 3.0×10^5 cm/sec. The results obtained here and by Merritt (35) were that, with this higher value of v_S, there was less attenuation of the magnitude response and less phase shift. This same effect (on a larger scale) was found when studying the fast group response, and as noted there, it is caused by the greater attenuation length of the neutron wave perturbation. Also, with this higher value of v_S, the inflection point, found previously at ~ 2000 rad/sec, in the magnitude response curves at detector positions D and E with the oscillator at positions 1 or 2 occurred at a higher frequency (~ 3500 rad/sec). This shows that the cause of this phenomenon is in the slow group; since the fast group response curves showed this behavior at the same frequency as the slow group response curves.

E. Dependence on Delayed Neutron Fraction

Inspection of the transfer function

$$\frac{\phi_o}{\Lambda}\left[\frac{j\omega + \lambda}{j\omega(j\omega + \beta/\Lambda)}\right] \quad ,$$

which was found by Danofsky and Uhrig (14) to be applicable to the UTR-10 reactor with no flux tilt, reveals that if β is increased the β/Λ frequency break of the magnitude response curve will occur at a higher frequency and the magnitude will be slightly less at frequencies less than β/Λ.

In order to determine whether or not the UTR-10 model developed here would show this effect, the value of β was increased to 0.0075. The results obtained predicted this effect exactly, which again shows that this model is giving results which are consistent with expected behavior.

F. Effect of Coupling Region Width

As the coupling region width was changed, the locations of detector positions C, D, and E were adjusted so that they always remained in the center of the coupling region, in the center of the north core tank, and 20 cm from the north core tank in the north reflector respectively.

The frequency response at detector positions A and B showed almost no change as the coupling region width was changed. The magnitude and phase of the frequency response

at detector positions C, D, and E as the coupling region width was increased from 25 to 75 cm are shown in Figures 14-19. In general, as the coupling region width increased there was a greater magnitude attenuation and phase shift.

As the coupling region width increases, the inflection point in the magnitude response curves at detector position D becomes more pronounced until, at a width of 75 cm, an actual sink occurs. Thus, whatever is the cause, this behavior is strongly dependent on the coupling region width. The magnitude response at detector position E is similar to that at D but is less pronounced. This indicates that the response at E is merely the attenuation of the effect originating in the north core.

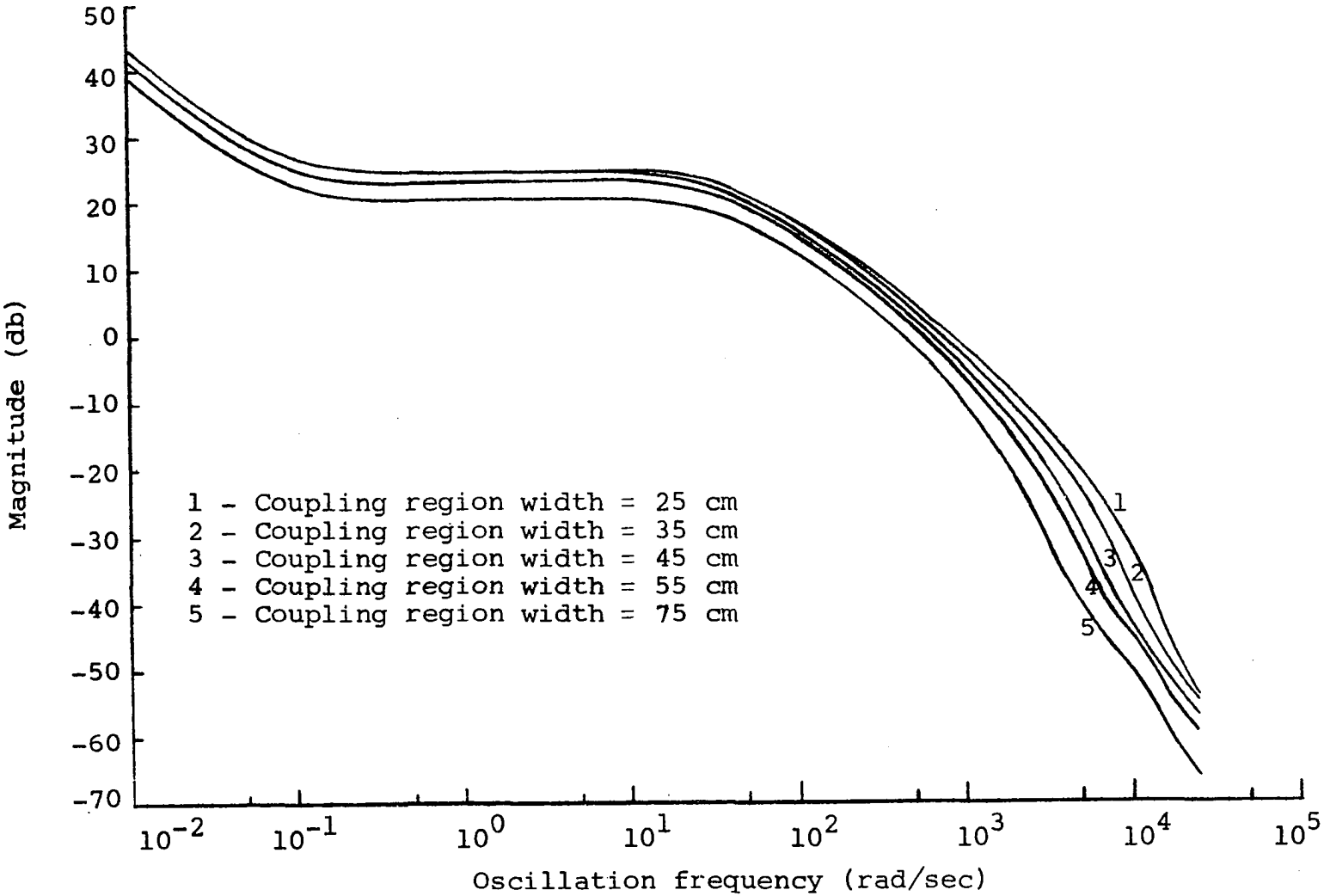

Figure 14. Magnitude of frequency response at position C, oscillator at position 2

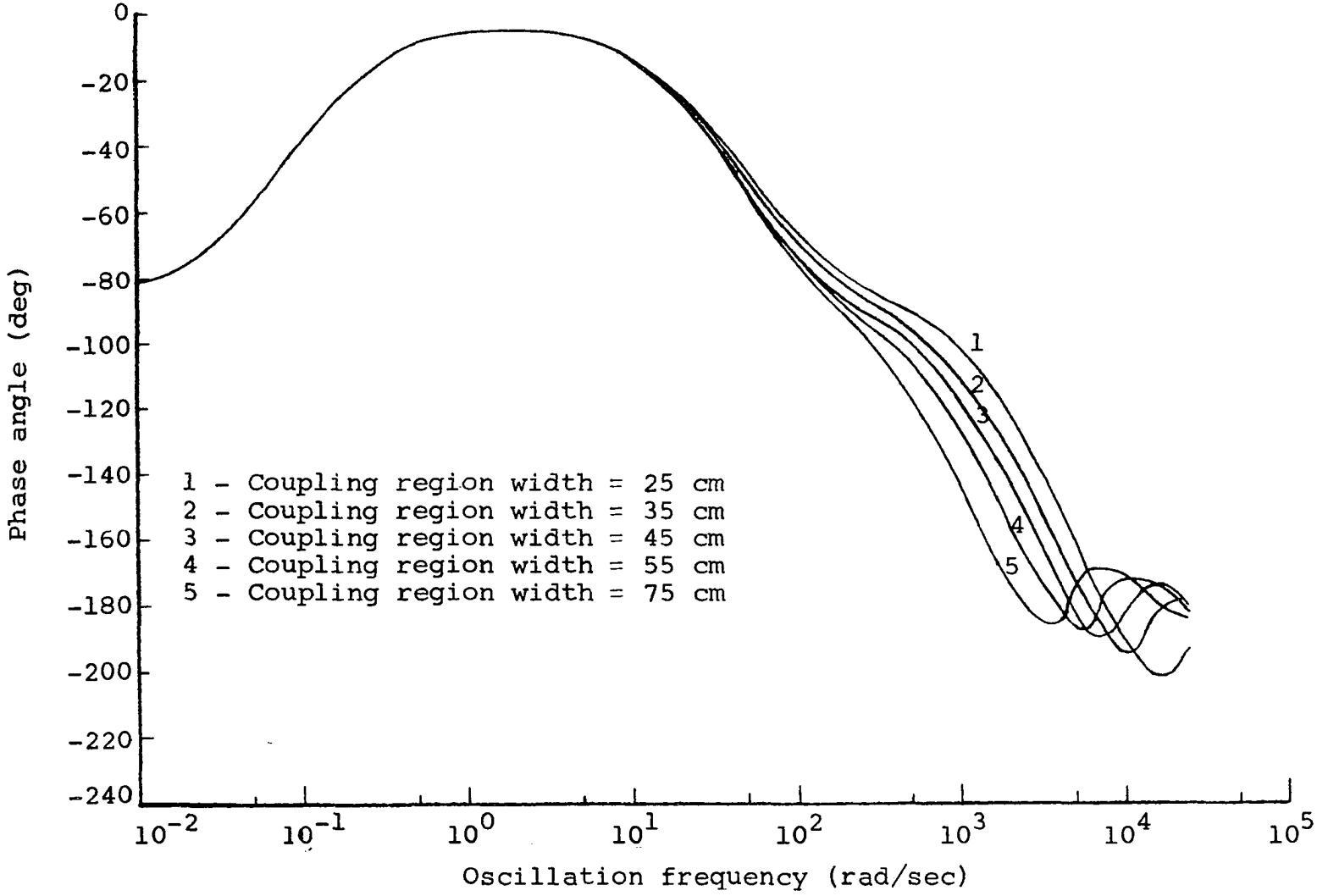

Figure 15. Phase of frequency response at position C, oscillator at position 2

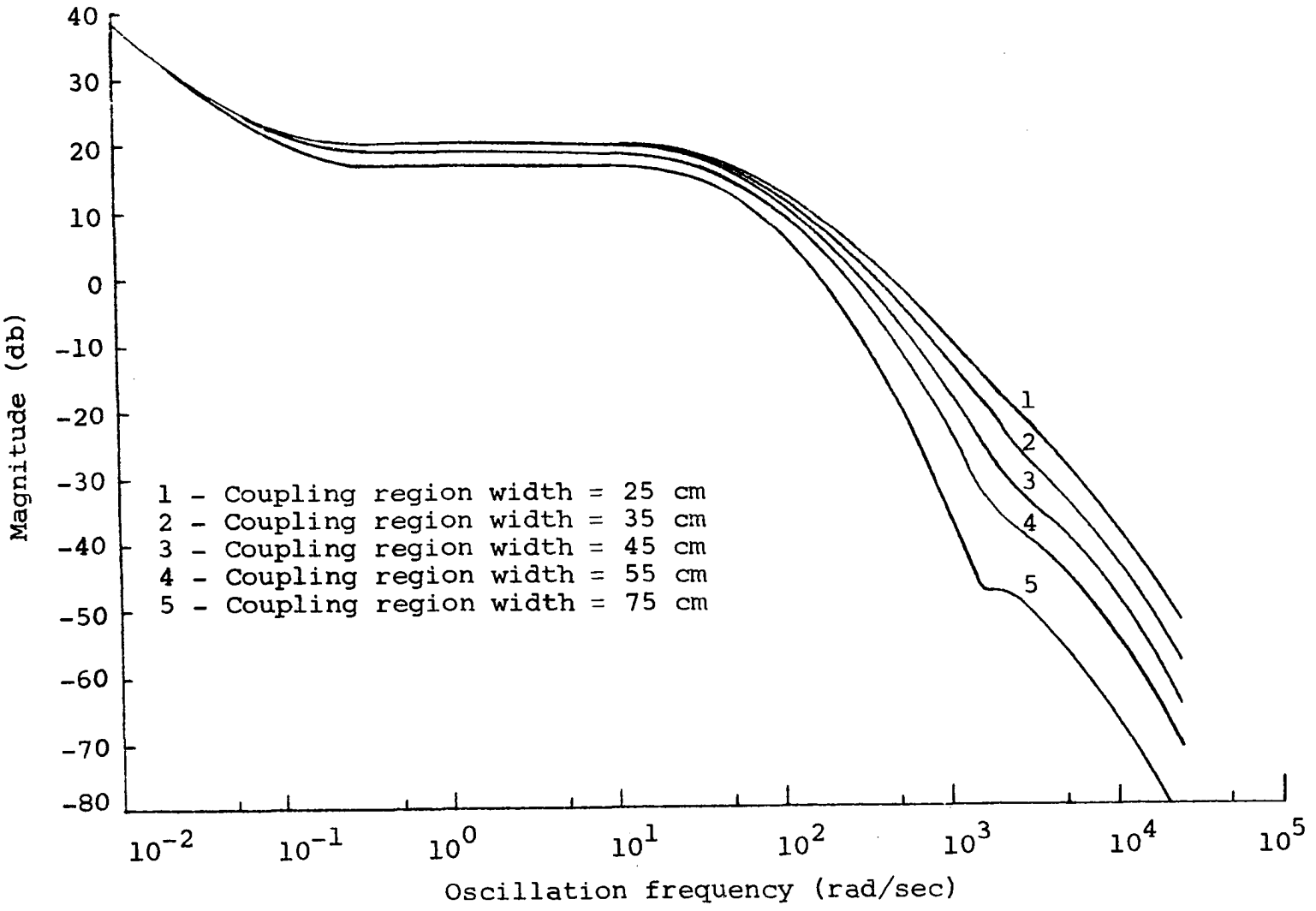

Figure 16. Magnitude of frequency response at position D, oscillator at position 2

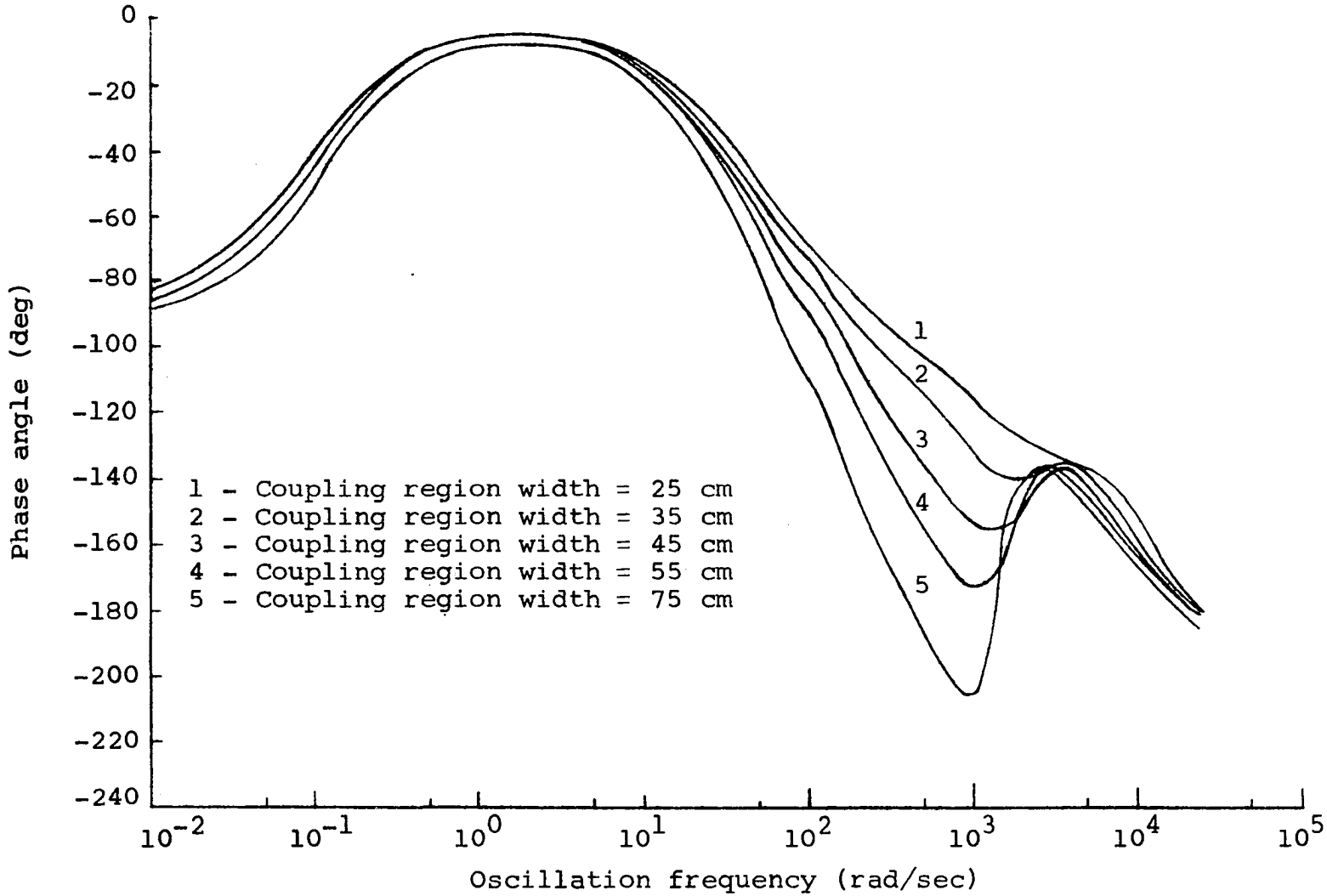

Figure 17. Phase of frequency response at position D, oscillator at position 2

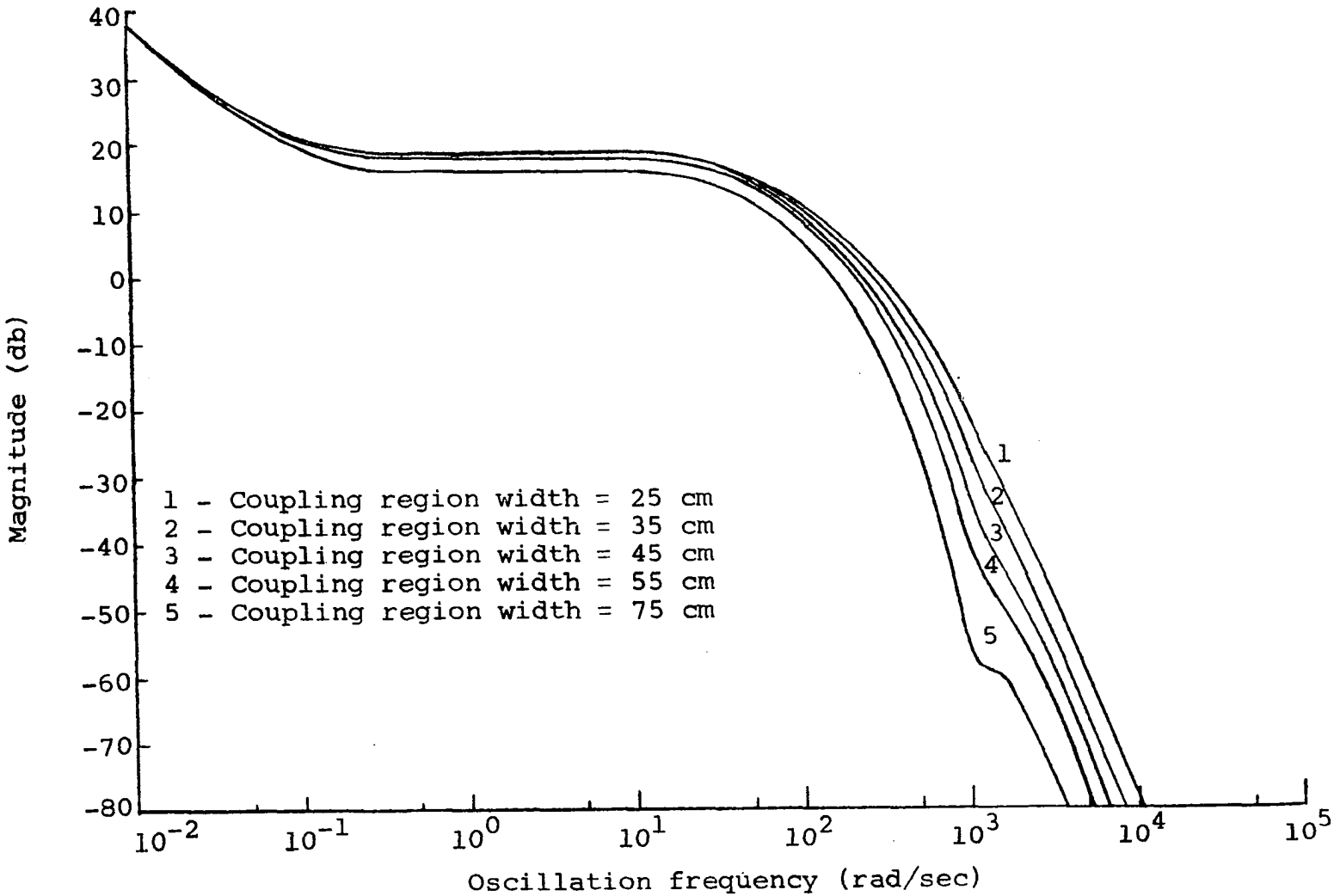

Figure 18. Magnitude of frequency response at position E, oscillator at position 2

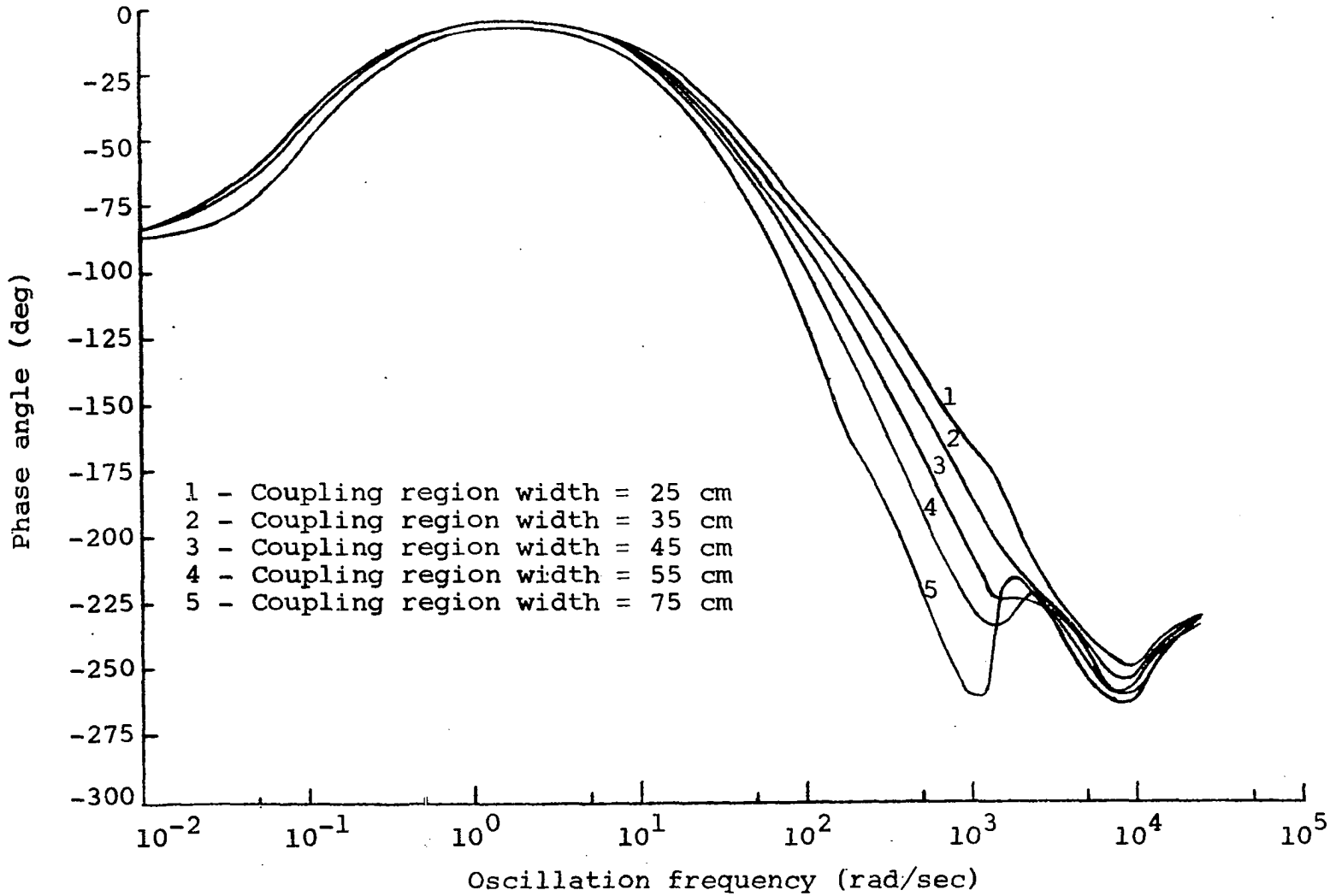

Figure 19. Phase of frequency response at position E, oscillator at position 2

VI. CONCLUSIONS

As a result of this study, the following conclusions can be drawn concerning the frequency response of a reactor:

1. The Green's function solution technique proposed here gives frequency response results which are consistent with expected behavior.
2. The frequency response of a reactor at low frequencies is essentially space-independent, but it is very sensitive to reactor criticality.
3. The magnitude and phase of the frequency response at or near the position of the oscillator exhibit a resonance effect at high frequencies.
4. The frequency response shows a greater magnitude attenuation and phase shift as the detector is moved away from the oscillator.
5. When the detector position is far from the oscillator, a consistent value of the β/Λ frequency break in the magnitude response curve is obtained.

The following conclusions apply specifically to a coupled-core reactor:

1. At positions far from the oscillator, the fast-neutron-group frequency response is dependent on the slow-neutron-group oscillation at that point instead of the fast-group perturbation from the oscillator.

2. A slower fast-neutron-group speed causes more phase shift as the detector is moved away from the oscillator and the frequency is increased.
3. At positions far from the oscillator, the frequency response is strongly dependent on the coupling region width.
4. For a fixed oscillator position, the frequency response shows definite spatial-dependent behavior at the different detector positions; and at a fixed detector position, the frequency response shows a definite dependence on the oscillator position.
5. With the model used in this study, inflection points occur in the magnitude response curves at detector positions D and E with the oscillator at positions 1 or 2 at a frequency of ~ 2000 rad/sec; and these inflection points become more pronounced as the coupling region width is increased. Increasing the slow-neutron-group speed shifts these inflection points to higher frequencies, which indicates that the inflection is a slow-group phenomenon; and since the inflection points occur only at positions D and E, this indicates that they are caused by an interaction between the two cores. The response at position E seems to be merely the attenuation of the effect originating in the north core.

VII. SUGGESTIONS FOR FURTHER WORK

The following suggestions are made for possible future work:

1. Extend the Green's function solution technique developed here to include more neutron energy groups. A possible means of doing this might be to use the concept of a Green's matrix (11).
2. Other parameters of the coupled-core reactor could be investigated for their effect on the frequency response, such as fuel enrichment and moderator material. Also, it would be interesting to examine the effects of greater coupling region widths on the sink effect.
3. Develop a model specifically for determining the frequency response near the frequency of the magnitude response inflection point.
4. Obtain experimental data to determine the spatially dependent frequency response at high frequencies (> 1000 rad/sec) in order to check the analytic results.
5. Apply the Green's function solution technique developed here to other reactor types, not necessarily only coupled-core reactors.

VIII. LITERATURE CITED

1. American Standard Company. Advanced Technology Laboratories Division. Operating manual for UTR-10 reactor. Mountain View, Calif., Author. 1959.

2. Ando, T. Spatial dependent transfer function of zero power reactors. Unpublished M.S. thesis. Ames, Iowa, Library, Iowa State University. 1964.

3. Avery, R. Theory of coupled reactors. Second International Conference on the Peaceful Uses of Atomic Energy 12: 182-191. New York, N.Y., United Nations. 1958.

4. Baldwin, G. C. Kinetics of a reactor composed of two loosely coupled cores. Nuc. Sci. and Eng. 6: 320-327. 1959.

5. Banks, N. E. and Blackshaw, G. L. Solution of the steady-state diffusion equation using Green's function. U.S. Army Materiel Command Report BRL-1374 [Ballistic Research Laboratories, Aberdeen Proving Ground, Md.]. 1967.

6. Belleni-Morante, A. Effect of first-flight neutrons on coupled reactor kinetics behaviour. J. of Nuc. Energy 21: 867-870. 1967.

7. Betancourt, J. M. Analysis of coupled core reactors using the natural mode approximation. Unpublished Ph.D. thesis. Ames, Iowa, Library, Iowa State University. 1968.

8. Carter, N. E. Solution of space-time kinetics equations for coupled-core nuclear reactors. Unpublished Ph.D. thesis. Ames, Iowa, Library, Iowa State University. 1967.

9. Carter, N. and Danofsky, R. The application of the calculus of variations and the method of Green's function to the solution of coupled core kinetics equations. In Chezem, C. G. and Köhler, W. H., editors. Conf. Coupled Reactor Kinetics, College Station, Texas, Jan., 1967. Pp. 249-269. College Station, Texas, The Texas A and M Press. 1967.

10. Churchill, R. V. Complex variables and applications. 2nd ed. New York, N.Y., McGraw-Hill Book Company, Inc. 1960.

11. Coddington, E. A. and Levinson, N. Theory of ordinary differential equations. New York, N.Y., McGraw-Hill Book Company, Inc. 1955.

12. Cohn, C. E., Johnson, R. J. and Macdonald, R. N. Calculating space-dependent reactor transfer functions using statics techniques. Nuc. Sci. and Eng. 26: 198-206. 1966.

13. Courant, R. and Hilbert, D. Methods of mathematical physics. Vol. 1. New York, N.Y., Interscience Publishers, Inc. 1953.

14. Danofsky, R. A. and Uhrig, R. E. The kinetic behavior of the coupled regions of the UTR-10 reactor. Nuc. Sci. and Eng. 16: 131-133. 1963.

15. Dougherty, D. E. and Shen, C. N. The space-time neutron kinetic equations obtained by the semi-direct variational method. Nuc. Sci. and Eng. 13: 141-148. 1962.

16. Foderaro, A. and Garabedian, H. L. A new method for the solution of group diffusion equations. Nuc. Sci. and Eng. 8: 44-52. 1960.

17. Foderaro, A. and Garabedian, H. L. Two group reactor kinetics. Nuc. Sci. and Eng. 14: 22-29. 1962.

18. Foulke, L. R. and Gyftopoulos, E. P. Application of the natural mode approximation to space-time reactor problems. Nuc. Sci. and Eng. 30: 419-435. 1967.

19. Glasstone, S. and Edlund, M. C. The elements of nuclear reactor theory. Princeton, N.J., D. VanNostrand Company, Inc. 1952.

20. Hansson, P. T. and Foulke, L. R. Investigations in spatial reactor kinetics. Nuc. Sci. and Eng. 17: 528-533. 1963.

21. Harrer, J. M., Boyar, R. E. and Krucoff, D. Transfer function of Argonne CP-2 Reactor. Nucleonics 10, No. 8: 32-36. 1952

22. Henry, A. F. and Curlee, N. J. Verification of a method for treating neutron space-time problems. Nuc. Sci. and Eng. 4: 727-744. 1958.

23. Hildebrand, F. B. Methods of applied mathematics. 2nd ed. Englewood Cliffs, N.J., Prentice-Hall, Inc. 1965.

24. Hoshino, T., Wakabayashi, J. and Hayashi, S. New approximate solution of space-and energy-dependent reactor kinetics. Nuc. Sci. and Eng. 23: 170-182. 1965.

25. Kaplan, S. The property of finality and the analysis of problems in reactor space-time kinetics by various modal expansions. Nuc. Sci. and Eng. 9: 357-361. 1961.

26. Kaplan, S. Space-time kinetics. In Radkowsky, A., editor. Naval reactor physics handbook. Vol. 1. Pp. 955-977. Washington, D.C., U.S. Govt. Print. Off. 1964.

27. Kaplan, S. and Bewick, J. A. Space and time synthesis by the variational method. U.S. Atomic Energy Commission Report WAPD-BT-28 [Westinghouse Electric Corp., Atomic Power Division, Pittsburg, Pa.]. 1963.

28. Kaplan, S., Henry, A. F., Margolis, S. G. and Taylor, J. J. Space-time reactor dynamics. Third International Conference on the Peaceful Uses of Atomic Energy 3: 41-50. New York, N.Y., United Nations. 1964.

29. Kaplan, S., Marlowe, O. J. and Bewick, J. Applications of synthesis techniques to problems involving time dependence. Nuc. Sci. and Eng. 18: 163-176. 1964.

30. Keepin, G. R. Physics of nuclear kinetics. Reading, Mass., Addison-Wesley Publishing Company, Inc. 1965.

31. Kobayashi, K. and Nishihara, H. Solution of group-diffusion equation using Green's function. Nuc. Sci. and Eng. 28: 93-104. 1967.

32. Kylstra, C. D. and Uhrig, R. E. Spatially dependent transfer function for nuclear systems. Nuc. Sci. and Eng. 22: 191-205. 1965.

33. Lewins, J. The approximate separation of kinetics problems into time and space functions by a variational principle. J. of Nuc. Energy 12, Part A: 108-112. 1960.

34. Loewe, W. E. Space dependent effects in the response of a nuclear reactor to forced oscillations. Nuc. Sci. and Eng. 21: 536-549. 1965.

35. Merritt, I. W. Spatially dependent frequency response of coupled-core reactors. Unpublished Ph.D. thesis. Ames, Iowa, Library, Iowa State University. 1968.

36. Pluta, P. R. Coupled core kinetic behavior. U.S. Atomic Energy Commission Symposium Series 7: 544-565. 1966.

37. Seale, R. L. Coupled core reactors. U.S. Atomic Energy Commission Report LAMS-2967 [Los Alamos Scientific Laboratory, Los Alamos, N. Mex.]. 1964.

38. Weaver, L. E. System analysis of nuclear reactor dynamics. New York, N.Y., Rowman and Littlefield, Inc. 1963.

39. Weinberg, A. M. and Schweinler, H. C. Theory of oscillating absorber in a chain reactor. Physical Review 74: 851-863. 1948.

40. Weinberg, A. M. and Wigner, E. P. The physical theory of neutron chain reactors. Chicago, Ill., The University of Chicago Press. 1958.

41. Wylie, C. R. Advanced engineering mathematics. 3rd ed. New York, N.Y., McGraw-Hill Book Company, Inc. 1966.

42. Yasinsky, J. B. On the application of time-synthesis techniques to coupled core reactors. Nuc. Sci. and Eng. 32: 425-429. 1968.

IX. ACKNOWLEDGMENTS

The author wishes to acknowledge his major professors, Dr. Glenn Murphy, Head of the Department of Nuclear Engineering and Dr. Richard A. Danofsky, for their support and interest throughout the course of this study, to acknowledge the support of the Department of Nuclear Engineering for a departmental assistantship, and to thank Dr. Danofsky for the many helpful suggestions and discussions during the time this study was performed.

The author also wishes to thank his parents, Mr. and Mrs. Edward C. Nodean, for their continued support and encouragement.

Finally, the author wishes to thank his wife, Deanna, who not only drew all the figures in this thesis, but also made all the work worthwhile.

X. APPENDIX A: DESCRIPTION OF THE UTR-10 REACTOR

The University Training Reactor-10 (UTR-10) is a light water moderated and cooled, graphite reflected, two-core reactor which is licensed for operation up to a power of 10 kilowatts.

The reactor is fueled with about 3 kilograms of fully enriched uranium (greater than 93% U-235) which is approximately evenly divided between the two cores. The uranium is arranged in fuel elements consisting of 12 aluminum-clad fuel plates each. There are 12 such fuel elements, which are positioned in two parallel core tanks (six elements in each tank) with the dimensions 5 in. by 20 in. by 24 in. These core tanks are embedded in a stack of graphite 44 in. by 56 in. by 48 in. and are separated by a graphite coupling region approximately 18 in. thick. Each core is itself subcritical, and criticality is achieved only by the exchange of neutrons between the cores through the coupling region. Deionized light water, which serves as both coolant and moderator, is circulated through each fuel element.

The reactor is controlled by varying the vertical position of four control rods containing boral (two safety rods, one shim rod, and one regulating rod) located in the graphite reflector adjacent to the core tanks. During normal operation the safety rods are fully withdrawn, and the power is controlled by positioning the shim and regulating

rods from the control console. When the reactor is scrammed, shutdown is achieved by the rapid injection of the safety and shim rods into the reflector and the rapid drainage of the water from the core tanks.

Figure A.1 illustrates the relative positions of the various reactor components and also shows some of the access ports to the core region.

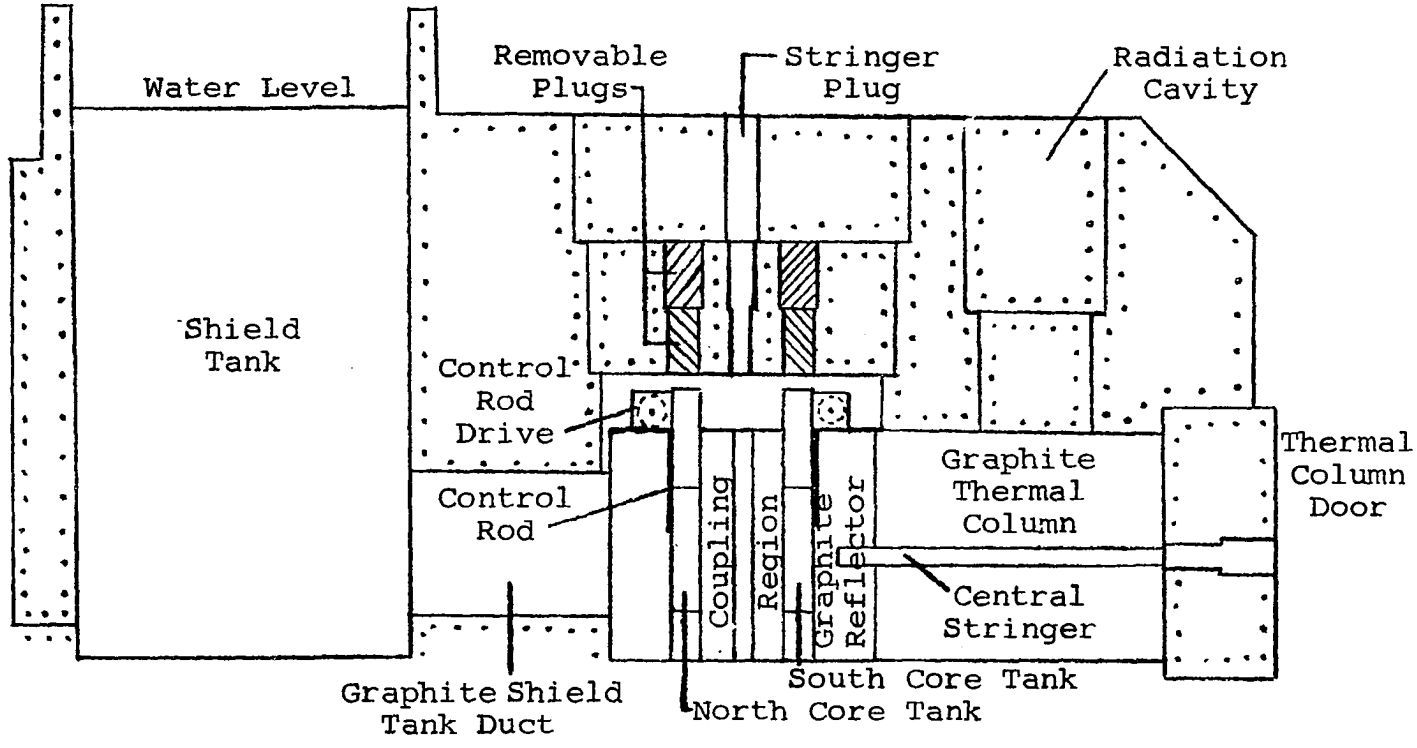

Figure A.1. UTR-10 reactor section

XI. APPENDIX B: DERIVATION OF THE TWO GROUP EQUATIONS FOR THE UTR-10 MODEL

To obtain the complex, two group equations for the UTR-10 model, the method of Cohn et al. (12) was used.

The basic two group diffusion equations with one group of delayed neutrons are (in one dimension)

$$D_F \frac{d^2}{dx^2}\phi_F - \Sigma_r \phi_F + \nu\Sigma_{fis}(1-\beta)\phi_S + \lambda C = \frac{1}{v_F}\frac{\partial \phi_F}{\partial t} \qquad (B.1)$$

$$D_S \frac{d^2}{dx^2}\phi_S - \Sigma_a \phi_S + \Sigma_r \phi_F = \frac{1}{v_S}\frac{\partial \phi_S}{\partial t} \qquad (B.2)$$

$$\nu\Sigma_{fis}\beta\phi_S - \lambda C = \frac{\partial C}{\partial t} \quad , \qquad (B.3)$$

where

ϕ_F = fast neutron flux

ϕ_S = slow neutron flux

D_F = fast diffusion coefficient

D_S = slow diffusion coefficient

Σ_r = fast removal cross section

Σ_a = slow absorption cross section

ν = number of neutrons per fission

Σ_{fis} = slow fission cross section

β = delayed neutron fraction

C = delayed neutron precursor density

λ = delayed neutron precursor decay constant

v_F = fast neutron group speed

v_S = slow neutron group speed.

Assuming a small perturbation in Σ_a,

$$\Sigma_a = \Sigma_{ao} - \Delta\Sigma_a \quad , \tag{B.4a}$$

then

$$\phi_F = \phi_{Fo} + \Delta\phi_F \quad , \tag{B.4b}$$

$$\phi_S = \phi_{So} + \Delta\phi_S \quad , \tag{B.4c}$$

and

$$C = C_o + \Delta C \quad . \tag{B.4d}$$

Σ_{ao}, ϕ_{Fo}, ϕ_{So}, and C_o are the steady-state values. Substituting Equations B.4 into Equations B.1, B.2, and B.3 yields

$$D_F\frac{d^2}{dx^2}(\phi_{Fo} + \Delta\phi_F) - \Sigma_r(\phi_{Fo} + \Delta\phi_F) + \nu\Sigma_{fis}(1-\beta)(\phi_{So} + \Delta\phi_S)$$

$$+ \lambda(C_o + \Delta C) = \frac{1}{v_F}\frac{\partial(\phi_{Fo} + \Delta\phi_F)}{\partial t} \tag{B.5}$$

$$D_S\frac{d^2}{dx^2}(\phi_{So} + \Delta\phi_S) - (\Sigma_{ao} - \Delta\Sigma_a)(\phi_{So} + \Delta\phi_S) + \Sigma_r(\phi_{Fo} + \Delta\phi_F)$$

$$= \frac{1}{v_S}\frac{\partial(\phi_{So} + \Delta\phi_S)}{\partial t} \tag{B.6}$$

$$\nu\Sigma_{fis}\beta(\phi_{So}+\Delta\phi_S) - \lambda(C_o+\Delta C) = \frac{\partial(C_o+\Delta C)}{\partial t} \quad . \qquad (B.7)$$

Noting that the steady-state parts of these equations sum to zero and assuming the product $\Delta\Sigma_a\Delta\phi_{So}$ is negligibly small results in

$$D_F\frac{d^2}{dx^2}\Delta\phi_F - \Sigma_r\Delta\phi_F + \nu\Sigma_{fis}(1-\beta)\Delta\phi_S + \lambda\Delta C = \frac{1}{v_F}\frac{\partial\Delta\phi_F}{\partial t} \qquad (B.8)$$

$$D_S\frac{d^2}{dx^2}\Delta\phi_S - \Sigma_{ao}\Delta\phi_S + \Delta\Sigma_a\phi_{So} + \Sigma_r\Delta\phi_F = \frac{1}{v_S}\frac{\partial\Delta\phi_S}{\Delta t} \qquad (B.9)$$

$$\nu\Sigma_{fis}\beta\Delta\phi_S - \lambda\Delta C = \frac{\partial\Delta C}{\partial t} \quad . \qquad (B.10)$$

Considering the case where the perturbation in Σ_a is provided by a neutron absorber oscillator so that $\Delta\Sigma_a$ can be considered sinusoidal and localized to a plane in the reactor, $\Delta\Sigma_a$ can be written as

$$\Delta\Sigma_a = \delta(x-x')\left|\bar{\Delta\Sigma}_a\right|e^{j\omega t} \quad ; \qquad (B.11a)$$

and thus,

$$\Delta\phi_F = \hat{\Delta\phi}_F(x,\omega)e^{j\omega t} \quad , \qquad (B.11b)$$

$$\Delta\phi_S = \hat{\Delta\phi}_S(x,\omega)e^{j\omega t} \quad , \qquad (B.11c)$$

and

$$\Delta C = \hat{\Delta C}(x,\omega)e^{j\omega t} \quad , \qquad (B.11d)$$

where

x' = location of oscillator in reactor,

ω = frequency of oscillator,

and $\hat{\Delta\phi}_F$, $\hat{\Delta\phi}_S$, and $\hat{\Delta C}$ are the complex amplitudes of $\Delta\phi_F$, $\Delta\phi_S$, and ΔC respectively. Substituting Equations B.11 into Equations B.8, B.9, and B.10 and dividing out the common factor $e^{j\omega t}$ yields

$$D_F\frac{d^2}{dx^2}\hat{\Delta\phi}_F - \Sigma_r\hat{\Delta\phi}_F + \nu\Sigma_{fis}(1-\beta)\hat{\Delta\phi}_S + \lambda\hat{\Delta C} = \frac{j\omega\hat{\Delta\phi}_F}{v_F} \qquad (B.12)$$

$$D_S\frac{d^2}{dx^2}\hat{\Delta\phi}_S - \Sigma_{ao}\hat{\Delta\phi}_S + \delta(x-x')|\Delta\Sigma_a|\phi_{So} + \Sigma_r\hat{\Delta\phi}_F = \frac{j\omega\hat{\Delta\phi}_S}{v_S} \qquad (B.13)$$

$$\nu\Sigma_{fis}\beta\hat{\Delta\phi}_S - \lambda\hat{\Delta C} = j\omega\hat{\Delta C} \quad . \qquad (B.14)$$

Solving Equation B.14 for $\hat{\Delta C}$ and substituting into Equation B.12 yields

$$D_F\frac{d^2}{dx^2}\hat{\Delta\phi}_F - \Sigma_r\hat{\Delta\phi}_F + \nu\Sigma_{fis}(1-\beta)\hat{\Delta\phi}_S + \frac{\nu\lambda\Sigma_{fis}\beta}{\lambda+j\omega}\hat{\Delta\phi}_S = \frac{j\omega\hat{\Delta\phi}_F}{v_F} \quad . \qquad (B.15)$$

Thus, the flux changes $\hat{\Delta\phi}_F$ and $\hat{\Delta\phi}_S$ can be determined by solving simultaneously Equations B.13 and B.15. However, since the UTR-10 has distinct fuel and moderator regions, the coefficients of $\hat{\Delta\phi}_F$ and $\hat{\Delta\phi}_S$ are variable. Thus, in order to retain the much simpler constant coefficient type of

equations, it is necessary to write a corresponding set of two equations pertaining only to the fuel regions and another set of two equations pertaining only to the moderator regions. In this way, solutions for the fast and slow flux changes in the fuel and moderator regions are obtained separately and then matched at the region interfaces with the continuity conditions on the fluxes and currents.

Letting the subscript f denote a fuel region and the subscript m denote a moderator region and considering the oscillator to be in a fuel region, the equations for the fuel regions are (from Equations B.13 and B.15)

$$D_{Ff}\frac{d^2}{dx^2}\hat{\Delta\phi}_{Ff} - \Sigma_{rf}\hat{\Delta\phi}_{Ff} + \nu\Sigma_{fis}(1-\beta)\hat{\Delta\phi}_{Sf} + \frac{\nu\lambda\Sigma_{fis}\beta}{\lambda + j\omega}\hat{\Delta\phi}_{Sf} = \frac{j\omega}{v_F}\hat{\Delta\phi}_{Ff} \qquad \text{(B.16)}$$

$$D_{Sf}\frac{d^2}{dx^2}\hat{\Delta\phi}_{Sf} - \Sigma_{aof}\hat{\Delta\phi}_{Sf} + \delta(x-x')\,|\bar{\Delta\Sigma}_{af}|\phi_{Sof} + \Sigma_{rf}\hat{\Delta\phi}_{Ff} = \frac{j\omega}{v_S}\hat{\Delta\phi}_{Sf} \quad ; \qquad \text{(B.17)}$$

and the equations for the moderator regions, where there is no production of neutrons, are

$$D_{Fm}\frac{d^2}{dx^2}\hat{\Delta\phi}_{Fm} - \Sigma_{rm}\hat{\Delta\phi}_{Fm} = \frac{j\omega}{v_F}\Delta\phi_{Fm} \qquad \text{(B.18)}$$

$$D_{sm}\frac{d^2}{dx^2}\hat{\Delta\phi}_{Sm} - \Sigma_{am}\hat{\Delta\phi}_{Sm} + \Sigma_{rm}\hat{\Delta\phi}_{Fm} = \frac{j\omega}{v_S}\hat{\Delta\phi}_{Sm} \quad . \qquad (B.19)$$

In order to account for neutron leakage through the top, bottom, and two sides of the reactor, the neutron fluxes are assumed to satisfy the wave equation in the y and z directions. Therefore, in the y direction,

$$\frac{d^2\phi}{dy^2} + B_y^2\phi = 0 \qquad \text{or} \qquad \frac{d^2\phi}{dy^2} = -B_y^2\phi \quad ;$$

and thus, the leakage in the y direction

$$D\frac{d^2\phi}{dy^2}$$

is equal to $-DB_y^2\phi$. Similarly, the leakage in the z direction is $-DB_z^2\phi$. Thus, the total transverse leakage is $-D(B_y^2 + B_z^2)\phi = -DB_t^2\phi$, where $B_t^2 = B_y^2 + B_z^2$ is the total transverse buckling. To account for this transverse leakage, the loss terms in Equations B.16-B.19 are modified as shown below:

$$D_{Ff}\frac{d^2}{dx^2}\hat{\Delta\phi}_{Ff} - (\Sigma_{rf} + D_{Ff}B_t^2)\hat{\Delta\phi}_{Ff} - \frac{j\omega}{v_F}\hat{\Delta\phi}_{Ff}$$

$$+ \nu\Sigma_{fis}(1-\beta)\hat{\Delta\phi}_{Sf} + \frac{\nu\lambda\Sigma_{fis}\beta}{\lambda + j\omega}\hat{\Delta\phi}_{Sf} = 0 \qquad (B.20)$$

$$D_{Sf}\frac{d^2}{dx^2}\Delta\hat{\phi}_{Sf} - (\Sigma_{aof} + D_{Sf}B_t^2)\Delta\hat{\phi}_{Sf} - \frac{j\omega}{v_S}\Delta\hat{\phi}_{Sf} + \Sigma_{rf}\Delta\hat{\phi}_{Ff}$$

$$+ \delta(x-x')|\Delta\bar{\Sigma}_{af}|\phi_{Sof} = 0 \qquad \text{(B.21)}$$

$$D_{Fm}\frac{d^2}{dx^2}\Delta\hat{\phi}_{Fm} - (\Sigma_{rm} + D_{Fm}B_t^2)\Delta\hat{\phi}_{Fm} - \frac{j\omega}{v_F}\Delta\hat{\phi}_{Fm} = 0 \qquad \text{(B.22)}$$

$$D_{Sm}\frac{d^2}{dx^2}\Delta\hat{\phi}_{Sm} - (\Sigma_{am} + D_{Sm}B_t^2)\Delta\hat{\phi}_{Sm} - \frac{j\omega}{v_S}\Delta\hat{\phi}_{Sm} + \Sigma_{rm}\Delta\hat{\phi}_{Fm} = 0 \,. \qquad \text{(B.23)}$$

With this formulation it is convenient to define "effective" cross sections; i.e.

$$\Sigma_{rfe} = \Sigma_{rf} + D_{Ff}B_t^2 \,,$$

$$\Sigma_{afe} = \Sigma_{aof} + D_{Sf}B_t^2 \,,$$

$$\Sigma_{rme} = \Sigma_{rm} + D_{Fm}B_t^2 \,,$$

and

$$\Sigma_{ame} = \Sigma_{am} + D_{Sm}B_t^2 \,.$$

With these definitions, Equations B.20-B.23 are the basic two group equations used to solve for the frequency response of the UTR-10.

XII. APPENDIX C: THE EQUIVALENCE OF THE FORMULATION USED IN THIS STUDY TO THE GREEN'S FUNCTION SOLUTION OF A FOURTH ORDER EQUATION

To simplify the arithmetic, consider a single-region, homogeneous reactor having a width of d cm and having a localized, sinusoidal oscillator located at some position x' within it. The relevant two-group equations to consider are then identical with Equation 46 (Section IV).

$$\frac{d^2}{dx^2}\hat{\Delta\phi}_F - K_F^2\hat{\Delta\phi}_F + H_1\hat{\Delta\phi}_S = 0 \qquad (C.1)$$

$$\frac{d^2}{dx^2}\hat{\Delta\phi}_S - K_S^2\hat{\Delta\phi}_S + H_2\hat{\Delta\phi}_F + \delta(x-x') = 0 \qquad (C.2)$$

The subscript f has been dropped since only a single-region reactor is being considered, but the terms have the same meaning as the corresponding ones in Equation 46.

Solving Equation C.1 for $\hat{\Delta\phi}_S$ yields

$$\hat{\Delta\phi}_S = \frac{1}{H_1}\left(-\frac{d^2}{dx^2}\hat{\Delta\phi}_F + K_F^2\hat{\Delta\phi}_F\right) . \qquad (C.3)$$

Substituting Equation C.3 into Equation C.2 and simplifying yields

$$\frac{d^4}{dx^4}\hat{\Delta\phi}_F - (K_F^2 + K_S^2)\frac{d^2}{dx^2}\hat{\Delta\phi}_F + (K_F^2K_S^2 - H_1H_2)\hat{\Delta\phi}_F - H_1\delta(x-x')=0. \qquad (C.4)$$

Equation C.4 is a fourth-order differential equation which can be solved by the Green's function technique outlined in Section II.

The first condition on the Green's function requires

$$\frac{d^4}{dx^4}G - (K_F^2 + K_S^2)\frac{d^2}{dx^2}G + (K_F^2K_S^2 - H_1H_2)G = 0 \quad . \tag{C.5}$$

Equation C.5 can be solved by ordinary techniques (41). Thus, assume solutions of the form

$$G_1 = Ae^{\alpha x} \quad , \quad x < x' \tag{C.6a}$$

$$G_2 = Ce^{\alpha x} \quad , \quad x > x' \quad , \tag{C.6b}$$

where G_1 and G_2 are the two parts of the Green's function. Substituting the expression for G_1 or G_2 into Equation C.5 and dividing out the common factor $Ae^{\alpha x}$ or $Ce^{\alpha x}$ yields

$$\alpha^4 - (K_F^2 + K_S^2)\alpha^2 + K_F^2K_S^2 - H_1H_2 = 0 \quad .$$

Thus,

$$\alpha^2 = 1/2[(K_F^2 + K_S^2) \pm \sqrt{(K_F^2 + K_S^2)^2 - 4(K_F^2K_S^2 - H_1H_2)}] \quad ,$$

and the four values of α are

$$\alpha_1 = [1/2(K_F^2 + K_S^2) + 1/2\sqrt{(K_F^2 + K_S^2)^2 - 4(K_F^2K_S^2 - H_1H_2)}]^{1/2} \tag{C.7}$$

$$\alpha_2 = -\alpha_1 \tag{C.8}$$

$$\alpha_3 = \left[1/2(K_F^2 + K_S^2) - 1/2\sqrt{(K_F^2 + K_S^2)^2 - 4(K_F^2K_S^2 - H_1H_2)}\right]^{1/2} \tag{C.9}$$

$$\alpha_4 = -\alpha_3 \ . \tag{C.10}$$

These values of α are identical with those found in Section IV (Equations 28-31). Thus, the solutions for G_1 and G_2 (Equations C.6) become

$$G_1 = A_1e^{\alpha_1 x} + A_2e^{\alpha_2 x} + A_3e^{\alpha_3 x} + A_4e^{\alpha_4 x} \ , \ x < x' \tag{C.11a}$$

$$G_2 = C_1e^{\alpha_1 x} + C_2e^{\alpha_2 x} + C_3e^{\alpha_3 x} + C_4e^{\alpha_4 x} \ , \ x > x' \ . \tag{C.11b}$$

The relevant homogeneous boundary conditions for Equation C.4 can be obtained from the homogeneous boundary conditions of Equations C.1 and C.2. These conditions are

$$\hat{\Delta\phi}_F(0) = 0 \tag{C.12a}$$

$$\hat{\Delta\phi}_S(0) = 0 \tag{C.12b}$$

$$\hat{\Delta\phi}_F(d) = 0 \tag{C.13a}$$

$$\hat{\Delta\phi}_S(d) = 0 \ . \tag{C.13b}$$

Substituting Equations C.12 into Equation C.1 yields

$$\frac{d^2}{dx^2}\Delta\hat{\phi}_F(0) = 0 \quad , \tag{C.14}$$

and substituting Equations C.13 into Equation C.1 yields

$$\frac{d^2}{dx^2}\Delta\hat{\phi}_F(d) = 0 \quad . \tag{C.15}$$

Thus, Equations C.12a, C.13a, C.14, and C.15 are the relevant homogeneous boundary conditions for Equation C.4.

The second condition on the Green's function requires

$$G_1(0) = 0 \tag{C.16}$$

$$\frac{d^2}{dx^2}G_1(0) = 0 \tag{C.17}$$

$$G_2(d) = 0 \tag{C.18}$$

$$\frac{d^2}{dx^2}G_2(d) = 0 \quad . \tag{C.19}$$

The third condition on the Green's function requires

$$G_1(x') = G_2(x') \tag{C.20}$$

$$\frac{dG_1(x')}{dx} = \frac{dG_2(x')}{dx} \tag{C.21}$$

$$\frac{d^2G_1(x')}{dx^2} = \frac{d^2G_2(x')}{dx^2} \quad . \tag{C.22}$$

The fourth condition on the Green's function requires

$$\frac{d^3G_2(x')}{dx^3} - \frac{d^3G_1(x')}{dx^3} = -1 \quad . \tag{C.23}$$

Equations C.16-C.23 are the eight conditions needed to solve for the eight independent constants in Equations C.11. Applying these eight conditions to Equations C.11 yields the following set of simultaneous, algebraic equations:

$$G_1(0) = A_1 + A_2 + A_3 + A_4 = 0 \tag{C.24}$$

$$\frac{d^2}{dx^2}G_1(0) = A_1\alpha_1^2 + A_2\alpha_2^2 + A_3\alpha_3^2 + A_4\alpha_4^2 = 0 \tag{C.25}$$

$$G_2(d) = C_1e^{\alpha_1 d} + C_2e^{\alpha_2 d} + C_3e^{\alpha_3 d} + C_4e^{\alpha_4 d} = 0 \tag{C.26}$$

$$\frac{d^2}{dx^2}G_2(d) = C_1\alpha_1^2e^{\alpha_1 d} + C_2\alpha_2^2e^{\alpha_2 d} + C_3\alpha_3^2e^{\alpha_3 d} + C_4\alpha_4^2e^{\alpha_4 d} = 0 \tag{C.27}$$

$G_1(x') = G_2(x')$ corresponds to

$$A_1e^{\alpha_1 x'} + A_2e^{\alpha_2 x'} + A_3e^{\alpha_3 x'} + A_4e^{\alpha_4 x'} = C_1e^{\alpha_1 x'} + C_2e^{\alpha_2 x'} + C_3e^{\alpha_3 x'} + C_4e^{\alpha_4 x'} \tag{C.28}$$

$\frac{dG_1(x')}{dx} = \frac{dG_2(x')}{dx}$ corresponds to

$$A_1\alpha_1 e^{\alpha_1 x'} + A_2\alpha_2 e^{\alpha_2 x'} + A_3\alpha_3 e^{\alpha_3 x'} + A_4\alpha_4 e^{\alpha_4 x'} =$$

$$C_1\alpha_1 e^{\alpha_1 x'} + C_2\alpha_2 e^{\alpha_2 x'} + C_3\alpha_3 e^{\alpha_3 x'} + C_4\alpha_4 e^{\alpha_4 x'} \qquad \text{(C.29)}$$

$\frac{d^2G_1(x')}{dx^2} = \frac{d^2G_2(x')}{dx^2}$ corresponds to

$$A_1\alpha_1^2 e^{\alpha_1 x'} + A_2\alpha_2^2 e^{\alpha_2 x'} + A_3\alpha_3^2 e^{\alpha_3 x'} + A_4\alpha_4^2 e^{\alpha_4 x'} =$$

$$C_1\alpha_1^2 e^{\alpha_1 x'} + C_2\alpha_2^2 e^{\alpha_2 x'} + C_3\alpha_3^2 e^{\alpha_3 x'} + C_4\alpha_4^2 e^{\alpha_4 x'} \qquad \text{(C.30)}$$

$\frac{d^3G_2(x')}{dx^3} - \frac{d^3G_1(x')}{dx^3} = -1$ corresponds to

$$C_1\alpha_1^3 e^{\alpha_1 x'} + C_2\alpha_2^3 e^{\alpha_2 x'} + C_3\alpha_3^3 e^{\alpha_3 x'} + C_4\alpha_4^3 e^{\alpha_4 x'} -$$

$$A_1\alpha_1^3 e^{\alpha_1 x'} - A_2\alpha_2^3 e^{\alpha_2 x'} - A_3\alpha_3^3 e^{\alpha_3 x'} - A_4\alpha_4^3 e^{\alpha_4 x'} = -1 \; . \qquad \text{(C.31)}$$

The solution of Equations C.24-C.31 will yield unique values for A_1-A_4 and C_1-C_4.

The solution for $\hat{\Delta\phi}_F$ is then [since the driving function is $-H_1\delta(x-x')$]

$$\hat{\Delta\phi}_F = -H_1 G \quad ,$$

or for $x < x'$,

$$\hat{\Delta\phi}_F = -H_1 G_1 \quad , \tag{C.32a}$$

and for $x > x'$,

$$\hat{\Delta\phi}_F = -H_1 G_2 \quad . \tag{C.32b}$$

From Equation C.3, the solution for $\hat{\Delta\phi}_S$ is:

for $x < x'$,

$$\hat{\Delta\phi}_S = \frac{d^2 G_1}{dx^2} - K_F^2 G_1 \quad , \tag{C.33a}$$

and for $x > x'$,

$$\hat{\Delta\phi}_S = \frac{d^2 G_2}{dx^2} - K_F^2 G_2 \quad . \tag{C.33b}$$

The formulation used in this study also starts with Equations C.1 and C.2. These equations can be rewritten in matrix form as follows,

$$\begin{bmatrix} \frac{d^2}{dx^2} - K_F^2 & H_1 \\ H_2 & \frac{d^2}{dx^2} - K_S^2 \end{bmatrix} \begin{bmatrix} \hat{\Delta\phi}_F \\ \hat{\Delta\phi}_S \end{bmatrix} + \begin{bmatrix} 0 \\ \delta(x-x') \end{bmatrix} = \begin{bmatrix} 0 \\ 0 \end{bmatrix} \quad , \tag{C.34}$$

which merely returns them to the form of Equation 46. Thus,

the Green's function solution to Equation C.34 is identical to that of Equation 46; that is (Equations 48 and 49),

for $x < x'$,

$$\hat{\Delta\phi}_F = G_{F1} = U_1 e^{\alpha_1 x} + U_2 e^{\alpha_2 x} + U_3 e^{\alpha_3 x} + U_4 e^{\alpha_4 x} \qquad \text{(C.35a)}$$

$$\hat{\Delta\phi}_S = G_{S1} = S_1 U_1 e^{\alpha_1 x} + S_2 U_2 e^{\alpha_2 x} + S_3 U_3 e^{\alpha_3 x} + S_4 U_4 e^{\alpha_4 x} , \qquad \text{(C.35b)}$$

and for $x > x'$,

$$\hat{\Delta\phi}_F = G_{F2} = V_1 e^{\alpha_1 x} + V_2 e^{\alpha_2 x} + V_3 e^{\alpha_3 x} + V_4 e^{\alpha_4 x} \qquad \text{(C.36a)}$$

$$\hat{\Delta\phi}_S = G_{S2} = S_1 V_1 e^{\alpha_1 x} + S_2 V_2 e^{\alpha_2 x} + S_3 V_3 e^{\alpha_3 x} + S_4 V_4 e^{\alpha_4 x} , \qquad \text{(C.36b)}$$

where the values of α are identical with Equations C.7-C.10 and S_1-S_4 are the coupling coefficients (Equation 33)

$$S_i = \frac{K_F^2 - \alpha_i^2}{H_1} , \quad i = 1,2,3,4 . \qquad \text{(C.37)}$$

Equations C.35 and C.36 fulfill the first condition on the Green's function.

Continuing with the method as proposed in this study, the second condition on the Green's function requires

$$G_{F1}(0) = 0 \qquad \text{(C.38)}$$

$$G_{S1}(0) = 0 \qquad \text{(C.39)}$$

$$G_{F2}(d) = 0 \tag{C.40}$$

$$G_{S2}(d) = 0 \quad . \tag{C.41}$$

The third condition on the Green's function requires

$$G_{F1}(x') = G_{F2}(x') \tag{C.42}$$

$$G_{S1}(x') = G_{S2}(x') \quad . \tag{C.43}$$

The fourth condition on the Green's function requires

$$\frac{dG_{F2}}{dx} - \frac{dG_{F1}}{dx} = 0 \tag{C.44}$$

$$\frac{dG_{S2}}{dx} - \frac{dG_{S1}}{dx} = -1 \quad . \tag{C.45}$$

Equations C.38-C.45 are the eight conditions needed to solve for the eight independent constants in Equations C.35 and C.36. Applying these eight conditions to Equations C.35 and C.36 yields the following set of simultaneous, algebraic equations:

$$G_{F1}(0) = U_1 + U_2 + U_3 + U_4 = 0 \tag{C.46}$$

$$G_{S1}(0) = S_1U_1 + S_2U_2 + S_3U_3 + S_4U_4 = 0 \quad . \tag{C.47}$$

Substituting the values of the S_i into Equation C.47 yields

$$\frac{K_F^2 - \alpha_1^2}{H_1}U_1 + \frac{K_F^2 - \alpha_2^2}{H_1}U_2 + \frac{K_F^2 - \alpha_3^2}{H_1}U_3 + \frac{K_F^2 - \alpha_4^2}{H_1}U_4 = 0 \quad . \tag{C.48}$$

Simplifying Equation C.48 yields

$$U_1\alpha_1^2 + U_2\alpha_2^2 + U_3\alpha_3^2 + U_4\alpha_4^2 = 0 \quad . \tag{C.49}$$

$$G_{F2}(d) = V_1 e^{\alpha_1 d} + V_2 e^{\alpha_2 d} + V_3 e^{\alpha_3 d} + V_4 e^{\alpha_4 d} = 0 \tag{C.50}$$

$$G_{S2}(d) = S_1 V_1 e^{\alpha_1 d} + S_2 V_2 e^{\alpha_2 d} + S_3 V_3 e^{\alpha_3 d} + S_4 V_4 e^{\alpha_4 d} = 0 \quad . \tag{C.51}$$

Substituting the values of the S_i into Equation C.51 and simplifying the result yields

$$V_1\alpha_1^2 e^{\alpha_1 d} + V_2\alpha_2^2 e^{\alpha_2 d} + V_3\alpha_3^2 e^{\alpha_3 d} + V_4\alpha_4^2 e^{\alpha_4 d} = 0 \quad . \tag{C.52}$$

$G_{F1}(x') = G_{F2}(x')$ corresponds to

$$U_1 e^{\alpha_1 x'} + U_2 e^{\alpha_2 x'} + U_3 e^{\alpha_3 x'} + U_4 e^{\alpha_4 x'} =$$

$$V_1 e^{\alpha_1 x'} + V_2 e^{\alpha_2 x'} + V_3 e^{\alpha_3 x'} + V_4 e^{\alpha_4 x'} \quad . \tag{C.53}$$

$G_{S1}(x') = G_{S2}(x')$ corresponds to (after substituting for the S_i and simplifying)

$$U_1\alpha_1^2 e^{\alpha_1 x'} + U_2\alpha_2^2 e^{\alpha_2 x'} + U_3\alpha_3^2 e^{\alpha_3 x'} + U_4\alpha_4^2 e^{\alpha_4 x'} =$$

$$V_1\alpha_1^2 e^{\alpha_1 x'} + V_2\alpha_2^2 e^{\alpha_2 x'} + V_3\alpha_3^2 e^{\alpha_3 x'} + V_4\alpha_4^2 e^{\alpha_4 x'} \quad . \tag{C.54}$$

$\frac{dG_{F2}(x')}{dx} - \frac{dG_{F1}(x')}{dx} = 0$ corresponds to

$$V_1\alpha_1 e^{\alpha_1 x'} + V_2\alpha_2 e^{\alpha_2 x'} + V_3\alpha_3 e^{\alpha_3 x'} + V_4\alpha_4 e^{\alpha_4 x'} -$$

$$U_1\alpha_1 e^{\alpha_1 x'} - U_2\alpha_2 e^{\alpha_2 x'} - U_3\alpha_3 e^{\alpha_3 x'} - U_4\alpha_4 e^{\alpha_4 x'} = 0 \quad . \text{(C.55)}$$

$\frac{dG_{S2}(x')}{dx} - \frac{dG_{S1}(x')}{dx} = -1$ corresponds to (after substituting for the S_i and simplifying)

$$V_1\alpha_1^3 e^{\alpha_1 x'} + V_2\alpha_2^3 e^{\alpha_2 x'} + V_3\alpha_3^3 e^{\alpha_3 x'} + V_4\alpha_4^3 e^{\alpha_4 x'} -$$

$$U_1\alpha_1^3 e^{\alpha_1 x'} - U_2\alpha_2^3 e^{\alpha_2 x'} - U_3\alpha_3^3 e^{\alpha_3 x'} - U_4\alpha_4^3 e^{\alpha_4 x'} = H_1 \quad . \quad \text{(C.56)}$$

This set of equations, Equations C.46, C.49, C.50, C.52-C.56, is identical in form to the set - Equations C.24-C.31 - except that Equation C.31 differs from Equation C.56 by a multiplicative factor of $-H_1$. This means that the set of constants U_i and V_i (i = 1,2,3,4) will differ from the set of constants A_i and C_i (i = 1,2,3,4) by only a multiplicative factor of $-H_1$.

Following the formulation in this study, for $x < x'$,

$$\hat{\Delta\phi}_F = G_{F1} \quad , \quad \text{(C.57a)}$$

and for $x > x'$,

$$\hat{\Delta\phi}_F = G_{F2} \quad , \quad \text{(C.57b)}$$

and since $G_{F1} = -H_1G_1$ and $G_{F2} = -H_1G_2$, the values for $\hat{\Delta\phi}_F$ found here are identical to those found from solving the fourth-order equation (Equation C.4).

Also, in this formulation, for $x < x'$,

$$\hat{\Delta\phi}_S = G_{S1} = S_1U_1e^{\alpha_1 x} + S_2U_2e^{\alpha_2 x} + S_3U_3e^{\alpha_3 x} + S_4U_4e^{\alpha_4 x}$$

or (substituting for the S_i)

$$\hat{\Delta\phi}_S = \frac{K_F^2 - \alpha_1^2}{H_1}U_1e^{\alpha_1 x} + \frac{K_F^2 - \alpha_2^2}{H_1}U_2e^{\alpha_2 x} + \frac{K_F^2 - \alpha_3^2}{H_1}U_3e^{\alpha_3 x} + \frac{K_F^2 - \alpha_4^2}{H_1}U_4e^{\alpha_4 x} , \qquad \text{(C.58a)}$$

and similarly, for $x > x'$,

$$\hat{\Delta\phi}_S = \frac{K_F^2 - \alpha_1^2}{H_1}V_1e^{\alpha_1 x} + \frac{K_F^2 - \alpha_2^2}{H_1}V_2e^{\alpha_2 x} + \frac{K_F^2 - \alpha_3^2}{H_1}V_3e^{\alpha_3 x} + \frac{K_F^2 - \alpha_4^2}{H_1}V_4e^{\alpha_4 x} . \qquad \text{(C.58b)}$$

The solution obtained for $\hat{\Delta\phi}_S$ from the fourth-order equation is (Equations C.33): for $x < x'$,

$$\hat{\Delta\phi}_S = \frac{d^2G_1}{dx^2} - K_F^2G_1$$

or (substituting for G_1 and carrying out the indicated operations)

$$\hat{\Delta\phi}_S = (\alpha_1^2 - K_F^2)A_1 e^{\alpha_1 x} + (\alpha_2^2 - K_F^2)A_2 e^{\alpha_2 x} + (\alpha_3^2 - K_F^2)A_3 e^{\alpha_3 x}$$

$$+ (\alpha_4^2 - K_F^2)A_4 e^{\alpha_4 x} \quad , \tag{C.59a}$$

and similarly, for $x > x'$,

$$\hat{\Delta\phi}_S = (\alpha_1^2 - K_F^2)C_1 e^{\alpha_1 x} + (\alpha_2^2 - K_F^2)C_2 e^{\alpha_2 x} + (\alpha_3^2 - K_F^2)C_3 e^{\alpha_3 x}$$

$$+ (\alpha_4^2 - K_F^2)C_4 e^{\alpha_4 x} \quad . \tag{C.59b}$$

As previously noted, the U_i and V_i differ from the A_i and C_i by only a multiplicative factor of $-H_1$. Thus, if $-H_1 A_i$ is substituted for U_i in Equation C.58a and $-H_1 C_i$ is substituted for V_i in Equation C.58b, it is easily seen that Equations C.58 and C.59 are identical.

Thus, the formulation used in this study is completely equivalent to the solution of the related fourth-order differential equation.